AIRBORNE NANOPARTICLES: GENERATION, CHARACTERIZATION, AND OCCUPATIONAL EXPOSURE

BEHNOUSH YEGANEH TALAB

Thesis submitted to the faculty of the Virginia Polytechnic Institute and State University in partial fulfillment of the requirements for the degree of

Master of Science

In

Environmental Engineering

Dr. Linsey Marr

Dr. Nancy Love

Dr. Peter Vikesland

March 14, 2007

Blacksburg, VA

Keywords: C_{60} fullerene, nanomaterials, nanoparticles, particle control, workplace exposure, occupational health

ABSTRACT

AIRBORNE NANOPARTICLES: GENERATION, CHARACTERIZATION, AND OCCUPATIONAL EXPOSURE

BEHNOUSH YEGANEH TALAB

Despite the rapid growth in nanotechnology, very little is known about the unintended health or environmental effects of manufactured nanomaterials. The development of nanotechnology risk assessments and regulations requires quantitative information on the potential for exposure to nanomaterials. In addition, to facilitate life-cycle assessments and inhalation toxicology studies, robust methods are needed to generate aerosolized engineered nanoparticles.

We conducted a set of field studies to measure the fine particle mass concentrations ($PM_{2.5}$) as well as nanoparticle number concentrations and size distributions in two nanomaterial manufacturing facilities. Measurements were performed near the reactor, in the breathing zone, and at a background site. Increases in $PM_{2.5}$ and particle number concentrations were associated with physical handling of nanomaterials. The highest $PM_{2.5}$ concentration observed was 2700 $\mu g\ m^{-3}$ during sweeping of the reactor in the commercial plant. In most cases, an increase in the number of sub-100 nm particles accounted for the increase in total number concentrations. The results of this research can be used to develop guidelines for workplace regulations to minimize workers' exposure to nanoparticles.

Furthermore, we used an atomizer to aerosolize C_{60} aggregates from a fullerene-water suspension. Measurement of particle size distributions and number concentrations showed that increasing the initial fullerene concentration resulted in increased number of aerosolized particles, while the average size of particles remained relatively constant. To return the aerosolized fullerenes into water, we passed the aerosol sample through an impinger. Reducing the flow rate through the impinger resulted in an increase in the collection efficiency of airborne nanoparticles.

ACKNOWLEDGEMENTS

I would like to express my deepest gratitude to my thesis advisor, Dr. Linsey Marr, for her guidance, advice, and support during my graduate studies and research work at Virginia Tech.

I would like to extend my appreciation to my advisory committee members, Dr. Nancy Love, Dr. Peter Vikesland, and Dr. John Little for their valuable advice, help, and time dedication.

This work was financially supported by a Virginia Tech ASPIRES grant, the National Science Foundation, and an Edna B. Sussman Foundation fellowship that are acknowledged with thanks.

I would also like to thank Julie Petruska, Jody Smiley, and Steve McCartney for their technical support. The time I spent at Virginia Tech would not be so enjoyable without the continuous help and support of my friends at Virginia Tech.

I treasure the consistent support, encouragement, and sustained love of my family; I could not have done it without them. Most importantly, very special thanks to my husband, Mohamadreza, for his invaluable help, encouragement, and support.

TABLE OF CONTENTS

LIST OF FIGURES

LIST OF TABLES

NOMENCLATURE AND ABBREVIATIONS

ELPI	Electrical low pressure impactor
$PM_{2.5}$	Fine particles of diameter 2.5 μm and less
SMPS	Scanning mobility particle sizer
SWCNT	Single-walled carbon nanotubes
TEM	Transmission Electron Microscopy
TNT-EMFs	Trimetallic nitride template endohedral metallofullerenes
η	Collection efficiency
d_p	Particle diameter

CHAPTER 1

INTRODUCTION

Concerns about the potential health risks and environmental impacts posed by engineered nanomaterials call for immediate action to ensure that the growing nanotechnology industry is safe and sustainable. This research aims to identify the potential exposure to airborne nanoparticles in nanotechnology workplaces and to demonstrate methods that can be used to study the physicochemical characteristics of nanomaterials in atmospheric and aquatic environments.

1.1 BACKGROUND

The rapid growth in the production of nanomaterials has raised concerns about the potential health and environmental hazards they might pose. Nanotechnology is expected to revolutionize materials, medicine, computing, machinery, and consumer products and to grow to a market of $1 trillion by 2015 (Roco 2005). Nanoparticles have at least one dimension of less than 100 nm, and due to their unique properties, these materials are being exploited in a growing number of applications (Borm 2002; Borm and Kreyling 2004; Colvin 2003; Gwinn and Vallyathan 2006).

Several recent studies have suggested that manufactured nanomaterials may have significant harmful effects on health. Studies of manufactured nanoparticles and naturally occurring ultrafine particles have shown that, when inhaled, smaller particles can be more toxic than a comparable mass of larger particles (Biswas and Wu 2005; Donaldson et al. 1998; Donaldson et

al. 2001; Donaldson et al. 2000; Maynard and Kuempel 2005; Oberdörster 2000; 2001; Oberdorster et al. 1995; Oberdörster et al. 2005; Peters et al. 1997; Pope et al. 2002; Tsuji et al. 2006). Additionally, surface area, chemical composition, solubility (Maynard and Kuempel 2005; Oberdörster et al. 2005; Tsuji et al. 2006), mobility (Wiesner et al. 2006), and number concentration (Anastasio and Martin 2001; Oberdörster et al. 1996) have been linked to health effects and toxicity. Some epidemiological studies also link extended exposure to ultrafine particles to pulmonary disease, cardiovascular health effects, and lung cancer mortality (Pope et al. 2002).

Carbon nanotubes have shown evidence of toxicity to mice, rats, and eukaryotic cells, compared to equivalent doses of quartz, which itself is considered a serious occupational health hazard (Jia et al. 2005; Lam et al. 2004; Warheit et al. 2004). Oberdörster (2004) reported that manufactured C_{60} fullerenes induced oxidative stress in the brains of fish, and Dhawan et al. (2006) showed that suspensions of C_{60} in water exhibited genotoxicity. Sayes et al. (2004) showed that under ambient conditions in water, fullerene can generate superoxide anions that might be responsible for membrane damage and subsequent cell death. Exposure to C_{60} also inhibited the growth and respiration rates of microbes (Fortner et al. 2005), although it demonstrated no toxic effects on eukaryotic cells (Jia et al. 2005).

However, to effectively and properly interpret toxicological data, it is essential to characterize the expected concentrations of engineered nanomaterials that may be present in the natural environment (Colvin 2003). Primary exposure to nanomaterials occurs during the manufacturing process (Wiesner et al. 2006). However, to date, only one study is known to have measured

airborne nanoparticles in the nanotechnology workplace (Maynard et al. 2004). This study found increased levels of aerosol mass concentrations during soot removal and cleaning of the reactor, but found no increase in the number concentration of submicron particles, i.e. only particles larger than 1000 nm were aerosolized.

In addition, the entire ecosystem can be exposed to engineered nanomaterials that are transported through air, water and soil (Colvin 2003). The physical characteristics of nanomaterials will impact their mobility and availability as well as their toxicity in each phase. Health and environmental risk assessments and life-cycle analyses of nanomaterial-based products require an improved understanding of the nature of nanomaterials in aquatic, atmospheric, and terrestrial environments (Wiesner et al. 2006). While some studies have characterized fullerenes in the liquid phase (Alargova et al. 2001; Andrievsky et al. 1995; Brant et al. 2005a; Brant et al. 2005b; Brant et al. 2005c; Deguchi et al. 2001), substantially fewer have considered their physical characteristics in aerosolized form.

Cross-media effects, e.g. between air and water, are often overlooked, yet need to be considered when assessing the transport, transformation, and fate of manufactured nanomaterials in the environment. Laboratory studies of cross-media effects on nanomaterials demand the ability to collect particles across the air-water interface in a controlled manner. It may also be advantageous to transfer airborne nanoparticles to liquid to facilitate chemical analysis (e.g. high-pressure liquid chromatography, spectrophotometry) in studies of nanomaterials. This approach also represents a potential control technology for removing highly concentrated nanoparticles from a gaseous waste stream.

A device known as an impinger is frequently used for trapping airborne particles in water, especially bioaerosols. In an impinger, an air stream is forced through a liquid bath, and impaction of airborne particles into the liquid and the bottom surface of the liquid reservoir as bubbles form is usually considered to be the main collection mechanism (Grinshpun et al. 1997). Studies evaluating the collection efficiencies of impingers have been mostly conducted with particles in the millimeter size range (Kim et al. 2002; Lin et al. 1997; Tseng and Li 2005; Willeke et al. 1998), while the collection efficiency of impingers for nanoscale particles has received less attention (Hogan et al. 2005; Kim et al. 2001; Spanne et al. 1999). Among those studies conducted in the nanoscale range, the collection efficiency for submicron particles was shown to be very low (Hogan et al. 2005; Spanne et al. 1999), suggesting that impingers are inadequate for collecting nanoscale particles. The full potential of the impinger, however, needs to be further explored for the study of nanoparticles.

This research study will concentrate on C_{60} fullerenes because of the large quantities being produced and potential persistence due to their chemical stability and small size. Aitken et al. (2006) reported that the Mitsubishi Corporation has a large-scale plant in Japan which claims to be producing 4-40 tons yr^{-1} of fullerenes.

1.2 PROBLEM DEFINITION

The quantification of health and environmental risks associated with nanomaterials, as well as life-cycle assessments of them, are critically needed for better understanding the nature of nanomaterial-based products (Wiesner et al. 2006). Given the limited data currently available on the exposure to airborne particles in the nanotechnology workplace, additional studies are

required to more fully characterize exposure to such particles. Furthermore, the physical characteristics of nanomaterials in the atmosphere, in terms of size distribution, concentration, and tendency to aggregate and deposit, play a key role in determining their longevity in natural environment, including aquatic, atmospheric and terrestrial systems. More information, with regards to both methods and characterization, is required for scientists to be able to predict nanoparticles' fate and transport in the atmosphere and to undertake toxicological inhalation studies. In addition, airborne nanoparticles need to be transferred into the liquid phase to facilitate chemical analysis and to study the cross-media effects of nanomaterials.

1.3 OBJECTIVES

The process of manufacturing and implementing nanomaterials in a vast number of applications can be better managed by understanding the exposure risk, physical and chemical characteristics, and transport routes of these particles in the environment. The overall goal of this research study was to elucidate the occupational exposure to manufactured nanoparticles, as well as to generate and characterize airborne nanoparticles. Three objectives were addressed:

- To assess the possible exposure to airborne nanoparticles released in the nanotechnology workplace.

To achieve this goal, we have conducted field measurements of mass concentrations of fine particulate matter ($PM_{2.5}$) as well as number concentrations and size distributions of nanoscale particles at two facilities where fullerenes are manufactured.

- To investigate the physical characteristics of laboratory-generated aerosolized nanoparticles.

To achieve this goal, we measured size distributions and number concentrations of airborne particles generated from aqueous-phase fullerene samples with varying initial concentrations.

- To optimize the collection efficiency of airborne nanoparticles in water.

We used a liquid impinger to collect airborne particles in water, and we calculated its efficiency in removing particles with diameters of less than 100 nm.

1.4 THESIS OUTLINE

This thesis is divided into five chapters. Chapter 2 reviews the literature to evaluate what is known about the exposure risk presented by nanoparticles in a nanomaterial manufacturing facility, the physical characteristics of fullerenes, and the collection of airborne particles in water. Fullerenes are emphasized as the nanomaterial of interest. At the end of second chapter, the results and shortcomings of the existing studies are described. Chapter 3 presents a comprehensive study of exposure to airborne nanoparticles during production of carbonaceous nanomaterials in the workplace. Chapter 4 includes the results of a laboratory-scale study to characterize the physical properties of aerosolized fullerene and to optimize nanoparticles' collection efficiency in water using an impinger. Chapter 5 provides the conclusions of this study and recommendations for future work.

CHAPTER 2

LITERATURE REVIEW

This chapter provides a review of related literature and identifies areas in which the research should be expanded. This chapter is divided into four main sections: exposure to airborne nanoparticles; characterization of aerosolized C_{60} fullerenes; collection of aerosolized nanoparticles in water using an impinger; and needs for further studies.

2.1 EXPOSURE TO AIRBORNE NANOPARTICLES

Although incidental exposure to high concentrations of nanomaterials is most likely to occur during the manufacturing process, very few studies have been conducted to evaluate the level of airborne particles in the nanotechnology workplace.

In the only known study involving manufactured nanomaterials, Maynard et al. (2004) used a condensation particle counter, optical particle counter, and scanning electron microscopy to characterize exposure to nanoparticles at four facilities producing single-walled carbon nanotubes (SWCNT). Aerosol mass concentrations were estimated at less that 53 $\mu g\ m^{-3}$ during handling of the unrefined SWCNT material, with increased levels found during soot removal and cleaning of the reactor. The number concentration of fine particles remained relatively constant throughout the course of the study. Furthermore, particle number and mass concentrations did not increase during any of the handling processes.

The aerosolization of submicron particles in the workplace is not limited to nanotechnology facilities. Considerably more studies have investigated exposure to airborne particles in other workplaces. For example, using a scanning mobility particle sizer (SMPS) and an electrical low pressure impactor (ELPI), Brouwer et al. (2004) observed an increase in number concentration of particles of less than 750 nm at a welding shop during and shortly after welding activities. In all such studies, however, the particles are a byproduct and not the main product of interest.

Uncertainty about the potential for exposure to manufactured nanoparticles in the workplace calls for additional research studies on this topic. This information is vital for scientists to conduct accurate risk assessments about nanotechnology, and for lawmakers to set air quality regulations in the nanotechnology workplace.

2.2 FULLERENE CHARACTERISTICS

In addition to the risk associated with the presence of nanoparticles in a nanomaterials manufacturing facility, there also exists the opportunity for wider exposure of the entire ecosystem to engineered nanomaterials through air, water, and soil if the nanomaterials escape into the environment. The physical characteristics of nanomaterials play a key role in determining their longevity in the natural environment.

To explore the physicochemical characteristics of nanomaterials in the aquatic environment, these materials must first be dispersed in water. Solvent exchange and direct dispersion of powdered C_{60} in water followed by prolonged mixing are the most common techniques that have been developed to produce stable dispersions of fullerenes in water. However, preparation of

fullerene suspensions by extended mixing of powdered C_{60} in water (aqu/nC_{60}) produces more polydisperse size distributions of colloidal fullerenes (Colvin 2003) compared to methods involving intermediate solvents, e.g. tetrahydrofuran to make THF/nC_{60}. Furthermore, aqu/nC_{60} is of special importance as it corresponds more closely to natural environmental transport scenarios (Dhawan et al. 2006). For this reason, this part of the literature review will only concentrate on the studies that have used extended mixing in water to prepare nC_{60} samples.

Brant et al. (2005a) showed that aqu/nC_{60} suspensions have size distributions in the range of 50 to 2000 nm, with a median value between 250 to 300 nm. The aqu/nC_{60} were not characterized by a single simple shape and instead appeared to form a film-like structure. Brant et al. (2005a) suggested that the surface chemistry of the aqu/nC_{60} may be similar to that of fullerol, which is hydroxylated, because of similar measured surface charges. This study also suggested that based on the contact angle with water, aqu/nC_{60} is hydrophilic.

In another set of studies performed by Brant et al. (2005b), suspensions of aqu/nC_{60} had a mean diameter of 180 nm. In this study, the authors suggested that C_{60} can acquire charge through hydroxylation of its surface either through adsorption of hydroxyl groups or hydrolysis, as the measured charge for aqu/nC_{60} was similar to that for hydroxylated C_{60} (fullerol). The results of this study imply that C_{60} molecules can become dispersed in water over time and become mobile as a result of charge acquisition. This result has important implications in determining the ability of colloidal C_{60} to transport and deposit on surfaces (Brant et al. 2005b).

In a study performed by Dhawan et al. (2006), extended mixing in water resulted in the

formation of relatively large (178 nm) and less negatively charged nC_{60} colloids, with spherical and hexagonal shapes, based on transmission electron microscopy (TEM) images. This study also found a small number of aggregated nC_{60} particles, in terms of intensity- and number-weighted size distributions, with diameters of 865 nm. When the stirring period was extended from 14 days to 11 months, particle diameters increased from 178 nm to 212 nm, and the absolute value of negative zeta potential also increased.

In further studies, Brant et al. (2006) analyzed unfiltered samples of aqu/nC_{60} and found that portions of the nC_{60} suspension were larger than the filter cutoff. There were two distinct peaks corresponding to median cluster sizes of 500 nm and 3 μm. The authors suggested that a sizable fraction of the nC_{60} or, possibly C_{60} crystallites, could be removed during the filtration step as a part of the preparation procedures. Brant et al. (2006) also showed that although pristine C_{60} molecules were strongly hydrophobic and uncharged, nC_{60}, regardless of the technique used to make them, were more hydrophilic and charged. Using the hydrocarbon partitioning test, the authors showed that aqu/nC_{60} primarily remained in the aqueous phase when exposed to a hydrocarbon such as dodecane. Additionally, reaggregation of smaller particles occurred after breakage in aqu/nC_{60}, resulting in the formation of the larger aggregates with a diameter of 160 nm. The authors also suggested that the size and formation of elementary particles was a function of the mixing conditions and the energy input to the dispersion.

To determine the environmental fate of nanomaterials, however, physicochemical characteristics of airborne nanoparticles must also be studied. Furthermore, definitive toxicity studies on the inhalation risk of nanoparticles will require that controlled amounts of aerosolized material be delivered to the test subjects. One challenge presented by nanoparticles, because of their large

surface area relative to mass, is their tendency to aggregate. The traditional method of administering powders for inhalation studies—mechanically dispersing the material into an air stream—does not provide sufficient force to deaggregate the particles into nanoscale sizes which are likely to be more relevant for engineered nanoparticles.

Sham et al. (2004) investigated aerosol delivery of nanoparticles to the lungs, with lactose as the carrier and gelatin and polybutylcyanoacrylate as the nanoparticles. Although the authors used the term "nanoparticles" in their work, the size of the particles they were considering was actually 200-300 nm, larger than the 100 nm cutoff typically used to define nanoparticles. Using a spray dryer with an air flow rate 11.67 L min^{-1}, the authors showed that both types of nanoparticles grew larger after being spray-dried due to coagulation. The mean size of particles increased by approximately 30% during this procedure.

One approach for generating and characterizing particles in the nanoscale range is to atomize engineered nanomaterials from their aqueous-phase suspensions. However, to the best of our knowledge, no one has yet generated airborne nanoparticles from engineered carbonaceous nanomaterials, C_{60} fullerene in our case, for characterization and toxicology studies.

2.3 COLLECTION EFFICIENCY OF FULLERENE IN WATER

One of the key steps in assessing the life cycle of manufactured nanomaterials, including their transport, transformation, and fate in natural environments, is the transfer of airborne particles to aquatic environments. Furthermore, it may be advantageous to transfer airborne nanoparticles to liquid to facilitate chemical analysis (e.g. high-pressure liquid chromatography,

spectrophotometry) and for studies of cross-media effects of nanomaterials. This approach also represents a potential control technology for removing highly concentrated nanoparticles from a gaseous waste stream.

Airborne particles naturally deposit to aquatic systems through gravitational settling, impaction, interception, or Brownian diffusion. The transfer process can be enhanced in the laboratory with the use of liquid impingers. Impingers are commonly used for trapping airborne particles in water, especially bioaerosols. In an impinger, an air stream is forced through a liquid bath, and impaction of airborne particles into the liquid and the bottom surface of the liquid reservoir as bubbles form is usually considered to be the main collection mechanism (Grinshpun et al. 1997). Previous work proposes that collection efficiencies in impingers should monotonically increase as a function of particles' inertia, which increases with particle size and velocity (Grinshpun et al. 1997; Kim et al. 2002; Lin et al. 1997). However, Grinshpun at al. (1997) showed that an increase in flow rate to levels above 10 L min^{-1} slightly decreased collection efficiency of an AGI-4 type of impinger, due to reaerosolization of some particles from the collection fluid.

However, this logic is only valid for larger particles. While impaction is ineffective for nanoscale particles, the main collection mechanism acting on them is diffusion through Brownian motion (Hogan et al. 2005), which increases with decreasing particle size. For these types of particles, a lower flow rate will provide smaller bubbles and a longer residence time inside the liquid reservoir, allowing a smaller diffusion pathlength and more time for the particles to diffuse into the body of water. In contrary, increasing the flow rate will eventually decrease the collection efficiency of nanoscale particles due to the larger bubble size and decrease in residence time

within the sampler. Of the few studies that have investigated impingers' effectiveness for nanoscale particles, all found very low collection efficiencies over the range of particle diameters considered.

Hogan et al. (2005) used a differential mobility analyzer and an ultrafine condensation particle counter to investigate the efficiencies of three commonly used types of impingers (AGI-30, SKC BioSampler, and a frit bubbler) for collecting particles smaller than 300 nm. Measurements were performed as a function of particle size, sample flow rate, and sampling time; and the results showed that none of the samplers were adequate for collecting submicron particles. At a flow rate of 12.5 L min^{-1}, the collection efficiency increased from ~6 to 30% as particle diameter decreased from 60 to 10 nm, due to the increasing diffusivities of smaller particles. In addition, the authors performed measurements with flow rates in the range of 3-15 L min^{-1} and showed that at lower flow rates, 25 nm particles were captured by Brownian motion. Increasing the flow rate decreased collection efficiency due to the shorter residence time within the sampler.

Spanne et al. (1999) used a differential mobility analyzer and an ultrafine condensation particle counter to determine the efficiency of an all-glass midget impinger for collection of submicron particles. The measurements were performed at flow rates of 0.7, 1.0, and 2.0 L min^{-1}; and very low collection efficiencies were found for all them. At the flow rate of 1.0 L min^{-1}, the efficiency was less than 20% for particles with diameters between 20 and 700 nm.

A versatile aerosol concentration enrichment system was developed by Kim at al. (2001) to study the collection efficiency of nanoscale particles. Very high collection efficiency was achieved

with this system; however, this method works on the principle of condensation growth of nanoscale particles to supermicron sizes, enabling effective trapping of these particles by an impinger. Modifying nanoparticles through condensational growth is not an option for studying their fate and transport in the environment.

Other factors have also been shown to impact the efficiency of a liquid impinger. Several studies showed that the overall collection efficiencies of liquid impingers decreased with sampling time, due to entrainment of already-collected particles by air bubbles passing through the liquid, evaporation losses, and reaerosolization (Hogan et al. 2005; Lin et al. 1997; Willeke et al. 1998). However, Liu at al. (1997) showed that the number of reaerosolized particles was less than 10% within the first hour of sampling. Lin et al. (1997) also suggested that the distance between the impingement nozzle and the bottom surface of the liquid reservoir could determine the cut-point size of collected particles. Again, this idea assumes that impaction is the dominant mechanism for collection and therefore applies only to larger particles. The authors also showed that the AGI-4 was more efficient in collecting submicron particles and showed less particle size dependence than the AGI-30. The number, e.g. 30, in the AGI impinger models is the distance in millimeters between the impingment nozzle and the bottom surface of the reservoir. Other studies showed that collection efficiency increased with the volume of collection fluid until all impacted particles were taken up by the fluid (Grinshpun et al. 1997; Lin et al. 1997). Increased particle hydrophilicity was also expected to increase the collection efficiency of impingers (Grinshpun et al. 1997; Tseng and Li 2005), probably due to a decrease in the rate of particle reaerosolization (Grinshpun et al. 1997).

Based on the literature review that we presented in this section, existing studies of impinger collection efficiencies have not considered flow rates less than 0.7 L min^{-1}.

2.4 RESULTS OF LITERATURE REVIEW AND NEEDS FOR FURTHER STUDIES

The literature review presented in this chapter provides background information with regards to exposure risk associated with engineered airborne nanoparticles in the workplace, physicochemical characteristics of nanomaterials in aquatic and atmospheric environments, and the potential for collecting airborne nanomaterials in the aquatic phase for toxicity and life-cycle assessments.

Given the limited data currently available on each of these subjects, additional studies are required to more fully characterize the exposure to such particles and to understand their physical characteristics in airborne form. Collection of airborne nanoparticles in aquatic media is an additional step needed for studying their fate and transport in the natural environment.

CHAPTER 3

EXPOSURE TO AIRBORNE NANOPARTICLES DURING PRODUCTION OF CARBONACEOUS NANOMATERIALS IN THE WORKPLACE

3.1 ABSTRACT

Background: Despite the rapid growth in nanotechnology, very little is known about the unintended health or environmental effects of manufactured nanomaterials. The development of nanotechnology risk assessments and regulations requires quantitative information on the potential for exposure to nanomaterials.

Objectives: We conducted a set of field studies to measure the concentrations and size distributions of airborne particles in two nanomaterial manufacturing facilities, a commercial plant and a university laboratory, that produce specialized fullerenes.

Methods: We measured fine particle mass concentrations ($PM_{2.5}$) as well as nanoparticle number concentrations and size distributions in three locations at each facility: near the reactor in which nanomaterials were generated, in the breathing zone of a technician working with the reactor, and at a background site.

Results: Increases in $PM_{2.5}$ and particle number concentrations were associated with physical handling of nanomaterials, especially near the reactor. The highest $PM_{2.5}$ concentration reported

by a DustTrak aerosol photometer was 2700 μg m^{-3} during sweeping of the reactor in the commercial plant. In most cases, an increase in the number of sub-30 nm particles accounted for the majority of the increase in total number concentrations.

Conclusions: Nanoparticles as small as 5 nm are suspended during the manufacture of fullerenes and may present an exposure risk to workers. The results of this and similar types of research can be used to develop guidelines for workplace regulations and to design methodologies for minimizing worker exposure.

3.2 INTRODUCTION

As the production of nanomaterials, defined as having at least one dimension of less than 100 nm, accelerates, the need for understanding exposure to nanoparticles and their health and environmental effects has become critically important. The unique properties of nanomaterials are being exploited to improve drug delivery devices, medical images, fuel cells, superconductors, photovoltaics, quantum computers, environmental remediation techniques, and consumer products (Borm 2002; Borm and Kreyling 2004; Colvin 2003; Gwinn and Vallyathan 2006). Nanotechnology is expected to revolutionize our lives while growing to a market of $1 trillion by 2015 (Roco 2005). Despite the rapid growth in nanotechnology, very little is known about the potential for exposure to manufactured nanomaterials.

Some studies have shown that, when inhaled, smaller particles can be more toxic than a comparable mass of larger particles of the same material (Donaldson et al. 1998; Donaldson et al. 2000; Oberdörster 2001; Peters et al. 1997; Pope et al. 2002). Additionally, surface area,

chemical composition, and solubility have been linked to health effects (Maynard and Kuempel 2005; Oberdörster et al. 2005; Tsuji et al. 2006). Several recent studies have suggested that manufactured nanomaterials may have significant deleterious effects on health. Carbon nanotubes showed evidence of toxicity to mice, rats, and eukaryotic cells, compared to equivalent doses of quartz, which itself is considered a serious occupational health hazard (Jia et al. 2005; Lam et al. 2004; Warheit et al. 2004). Oberdörster (2004) reported that manufactured C_{60} fullerenes induced oxidative stress in the brains of fish, and Dhawan et al. (2006) showed that suspensions of C_{60} in water exhibited genotoxicity. Exposure to C_{60} also inhibited the growth and respiration rates of microbes (Fortner et al. 2005), although it had no toxic effects on eukaryotic cells (Jia et al. 2005).

Exposure to high levels of nanomaterials is most likely to occur during manufacturing (Wiesner et al. 2006). However, to date, only one study is known to have measured airborne nanoparticles in the nanotechnology workplace. Maynard et al. (2004) used a condensation particle counter, optical particle counter, and scanning electron microscope to characterize exposure to nanoparticles at four facilities producing single-walled carbon nanotubes (SWCNT). Aerosol mass concentrations were estimated at less than 53 $\mu g\ m^{-3}$ during handling of the unrefined SWCNT material, with increased levels found during soot removal and cleaning of the reactor. Researchers did not observe an increase in the number concentration of submicron particles during the handling of materials, but particles larger than 1 μm may have been released.

Given the limited data currently available on exposure to airborne particles in the nanotechnology workplace, additional studies are needed to more fully characterize exposure to

such particles. Size is especially important because individual nanoparticles, as small as 1 nm, are likely to aggregate (van Poppel et al. 2005), and the resulting size of aerosolized particles will determine their fate in the respiratory tract, if inhaled, and in the environment. While diffusion and gravitational settling act to remove the smallest and largest particles, those in the range of approximately 100-1000 nm can remain airborne for weeks.

Fullerenes are of interest because of the large quantities being produced and their demonstrated toxicity. The Mitsubishi Corporation has a large-scale plant in Japan which claims to be producing 4-40 tons yr^{-1} of fullerenes (Aitken et al. 2006). While no single study can definitively assess the exposure risk presented by airborne particles in the nanotechnology workplace, the goal of this research is to provide an important set of measurements that will contribute to the understanding of such exposures and that will guide the design of future studies. To achieve this goal, we have conducted field measurements of fine particulate matter (aerodynamic diameter < 2.5 μm, $PM_{2.5}$) mass concentrations as well as number concentrations and size distributions of nanoscale particles at two facilities where fullerenes are manufactured. Such research is needed to guide the development of regulations that will protect human health and the environment from any potential harm posed by nanotechnology.

3.3 MATERIALS AND METHODS

Facilities. The study was conducted in 2005 and 2006 at a commercial manufacturing plant and a university laboratory. The production division of the commercial facility consists of two adjacent rooms, each approximately 20 m^2, connected by a short hallway. Four reactors are located in each room, but only two reactors in one of the rooms were functional at the time of

sampling. Each reactor is enclosed in its own specialized fume hood to minimize worker exposure to particles. The fume hood has a plastic shield covering its front face, and workers access the reactors through two openings in the shield. The exact dimensions of the fume hood and shield are considered proprietary. The fume hood exhaust is treated by a bag-house filtration system designed to remove over 99% of nanoparticles before exiting to the atmosphere.

The university laboratory houses one reactor, which sat on a bench top in 2005 and was not enclosed. In 2006, the reactor was moved inside a large 4.88 m × 4.88 m × 4 m acrylic enclosure with an open top, essentially a room within a room. Four ceiling-mounted vacuum ventilation ducts are located in the reactor enclosure, with one hanging ~0.5 m immediately above the reactor opening.

Production process. Both facilities use the same methods to produce trimetallic nitride template endohedral metallofullerenes (TNT-EMFs) (Stevenson et al. 1999), which are extracted from the raw soot produced from graphite rods in electric-arc reactors. The precise reactor dimensions and nanomaterial production rates are considered proprietary. Both facilities introduced larger reactors in 2006, and production rates nearly doubled compared to 2005.

Raw soot in each of the manufacturing facilities is produced in batches 3-5 times a day. Each production run lasts 90-120 min and includes three steps: arc reaction, sweeping, and optional vacuuming. After placing the rods inside the reactor, a technician seals the reactor and subjects it to vacuum pressure. The ignition of an electric arc across two graphite rods results in the volatilization of the graphite and the production of raw soot containing carbonaceous

nanomaterials. At the end of the arc reaction, which lasts 60-90 min, the technician opens the reactor lid and sweeps out raw soot into a funnel and jar using a scoop and a brush. The sweeping process usually takes 3-20 min.

At the end of the final run each day in the commercial manufacturing plant, the reactors are completely swept and vacuumed using a high efficiency particulate air (HEPA) vacuum cleaner to remove residual soot from the reactor chamber, brushes, funnel, and inside surfaces of the fume hood. The vacuuming process usually takes 5-15 min. In the university laboratory, vacuuming takes place only when a new type of graphite rod is introduced, which does not necessarily occur every day. During the course of the study, we observed only one vacuuming event in the lab.

Field sampling. Measurements were conducted as part of an exploratory pilot study over four days in August and October 2005 and as part of a more comprehensive investigation over seven days in June, July, and August 2006. In total, we monitored 12 production runs at the commercial plant and 19 in the university laboratory.

At the commercial manufacturing plant, measurements were collected in three different locations: (1) near the reactor (~10 cm from the reactor's opening) and inside the fume hood, (2) in the breathing zone of technicians working with the reactor, just outside the fume hood and 150 cm above the floor, and (3) at a background location, 1-2 m behind the technicians and 150 cm above the floor. We also measured particle concentrations in ambient air outside the commercial plant. Measurements were collected at the same three types of locations in the university lab.

Particle characterization. In this study, we measured $PM_{2.5}$ mass concentrations and submicron particle size distributions. A light-scattering aerosol photometer (TSI DustTrak 8520, Shoreview, MN) was used to monitor $PM_{2.5}$ mass concentrations. The method is only sensitive to particles larger than 100 nm. However, as mass scales with diameter cubed, smaller particles are not expected to contribute much to mass concentrations. The DustTrak recorded $PM_{2.5}$ at 1-s intervals in all sampling locations, except in the background location of the university lab, where $PM_{2.5}$ was recorded at 10-s intervals. On two occasions, we were able to borrow an identical DustTrak and used it to monitor $PM_{2.5}$ continuously at the background locations at 10-s intervals. Both instruments had been factory calibrated by the manufacturer within the past year. In August 2006, the two DustTraks were co-located in the commercial plant for 8.5 hours, and one of them was found to read 1.099 times lower than the one most recently calibrated in May 2006. Hence, all results from the second DustTrak have been scaled up by a factor of 1.099. Both DustTraks were zero calibrated at the beginning of each sampling trip, and their inlet flow rates were adjusted to the recommended value of 1.7 L min^{-1}.

Additionally, we collected $PM_{2.5}$ samples for gravimetric analysis on 47 mm PTFE filters (Pall Corporation, East Hills, NY) with glass fiber backup filters for support (SKC Inc., Eighty Four, PA). The sampling system used a flow rate of 10 L min^{-1} and a cyclone with a 2.5 μm cut-point (URG 2000-30EN, Chapel Hill, NC). We collected two filter samples over durations of 16 and 18 h at the background location in the commercial plant, co-located with a DustTrak. Filters were wrapped in aluminum foil and stored in a refrigerator until they could be weighed. The filters were conditioned at constant temperature and humidity for 24 h and weighed before and after sampling.

Because the DustTrak uses the light scattering method, its calibration is specific to the chemical composition and size distribution of the aerosol being measured. The factory calibration uses Arizona test dust, which is intended to be representative of a variety of ambient atmospheric aerosols. The ratios of DustTrak $PM_{2.5}$ to gravimetric $PM_{2.5}$ were 0.92 and 1.27 for our two filters. Because the results do not conclusively suggest that DustTrak readings should be corrected upward or downward, and to facilitate comparisons between the data presented here and the results of other studies using this instrument, we have decided not to adjust the $PM_{2.5}$ measurements shown in this work.

Particle size distributions were measured in situ using a scanning mobility particle sizer (TSI SMPS 3936) equipped with a nano or long differential mobility analyzer (NDMA, LDMA) and an ultrafine condensation particle counter (TSI 3025A). The NDMA allows measurement of particles with mobility diameters of 3-160 nm, and the LDMA covers a range of 14-673 nm. A single scan over the full range of particle sizes takes 120 s.

3.4 RESULTS

Mass and number concentrations. Figure 3.1 and the supplemental material present average $PM_{2.5}$ mass concentrations by location and activity in the commercial manufacturing facility in 2005. On 4 August, concentrations in the breathing zone and background were similar during all activities, and those near the reactor were higher, especially during sweeping. On 9 August, average $PM_{2.5}$ concentrations were lower at all locations compared to 4 August; and among the three locations, they were lowest in the breathing zone.

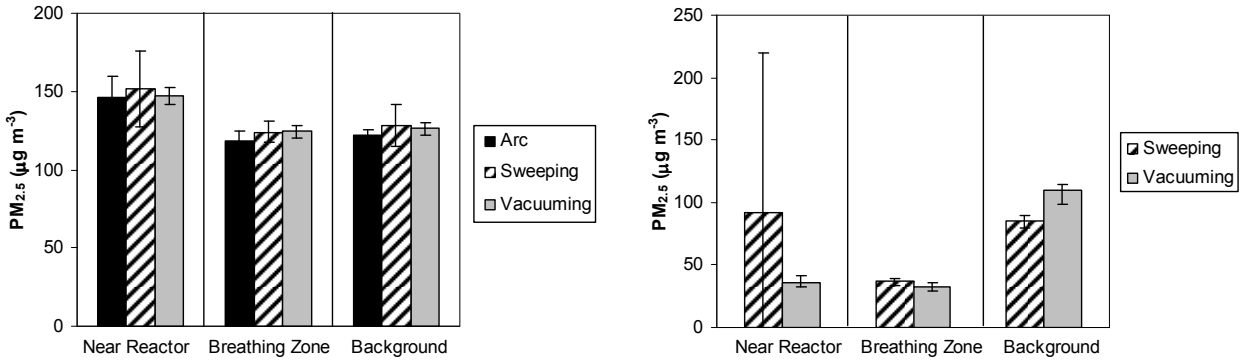

Figure 3.1. Average and standard deviation of 1-s $PM_{2.5}$ measurements at the commercial plant on 4 and 9 August 2005.

Near the reactor, concentrations were significantly higher and more variable during sweeping than during vacuuming. Due to concerns about power surges during arc reaction and potential damage to the sampling equipment, no monitoring was conducted during this procedure on the second day of sampling (9 August 2005).

Figure 3.2 shows time series of number concentrations of 14-673 nm particles as well as mass concentrations of $PM_{2.5}$ at three locations in the commercial manufacturing facility in 2006. Each panel in Figure 2 shows one complete production run consisting of arc reaction and sweeping. Vacuuming was performed twice, once at the beginning of measurements in the near reactor location and once at the end of measurements at the background site. Bars across the top of each panel indicate the duration of each activity. Number concentrations of particles smaller than 30 nm, between 30 and 100 nm, and larger than 100 nm have been also plotted separately to show the contribution of each size range to the total number concentration. Peaks in $PM_{2.5}$ and/or total number concentration usually occurred simultaneously: after vacuuming and during sweeping in the near reactor location, right before sweeping in the breathing zone, and before sweeping and

after vacuuming in the background. On three occasions, at 9:11, 13:22, and 15:43, $PM_{2.5}$ increased without a corresponding increase in total sub-673 nm particle number.

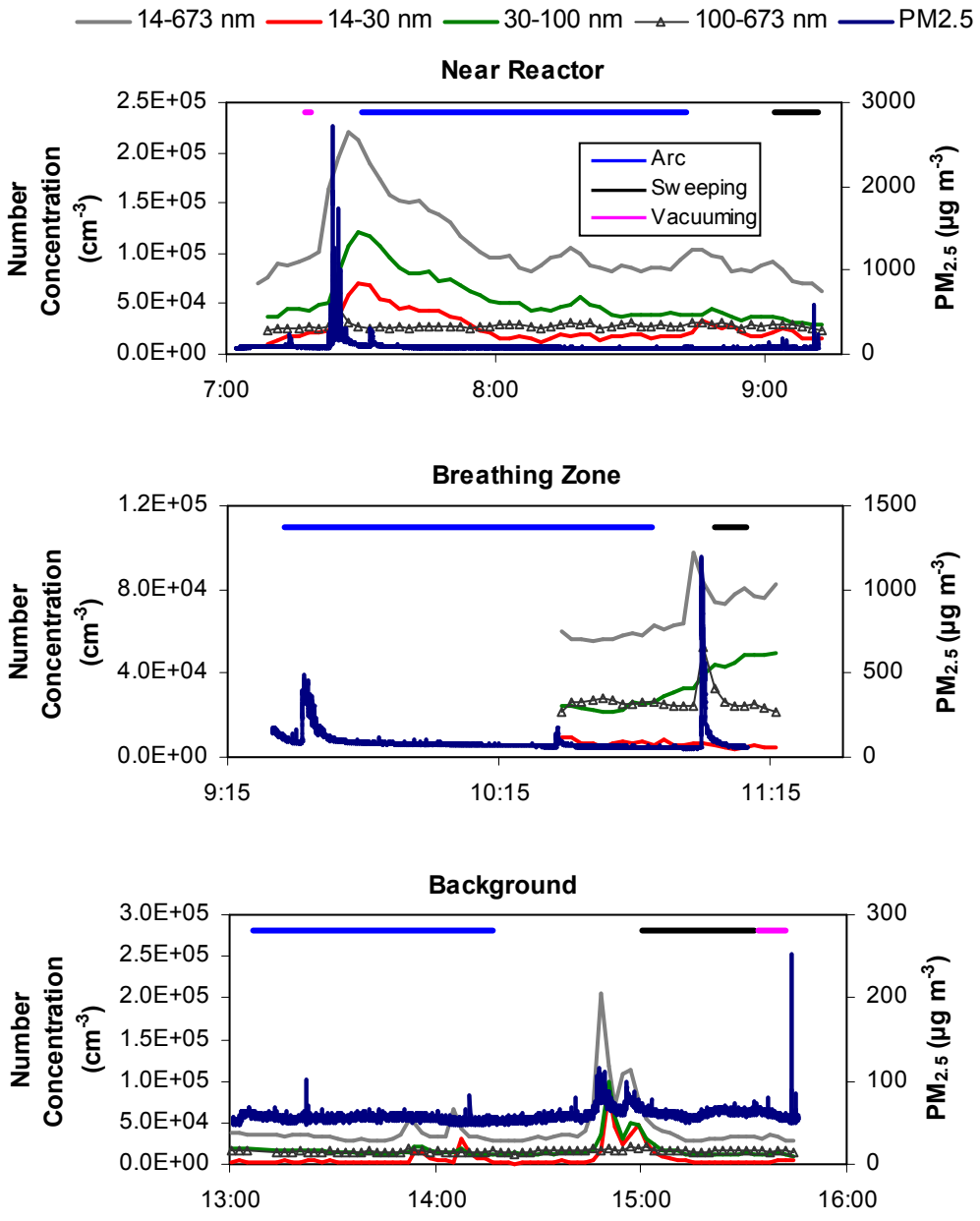

Figure 3.2. Particle number concentration and $PM_{2.5}$ time series in the commercial manufacturing facility on 25 July 2006, with the duration of production activities indicated by the bars across the top of each panel. Number concentrations are shown as the total between 14-673 nm and as subsets of this range.

Figure 3.3 illustrates $PM_{2.5}$ mass concentrations measured in the background in the commercial plant during the entire workday, the same day as shown in Figure 3.2. The first vacuuming event and first two sweeping events were immediately followed by large increases in $PM_{2.5}$. Figure 3.4 shows outdoor $PM_{2.5}$ and number concentrations measured on the same day between 11:27 and 12:45. The average $PM_{2.5}$ and sub-673 nm number concentration were 68.7 ± 14.6 µg m^{-3} and 1×105 ± 3×104 cm^{-3}, respectively.

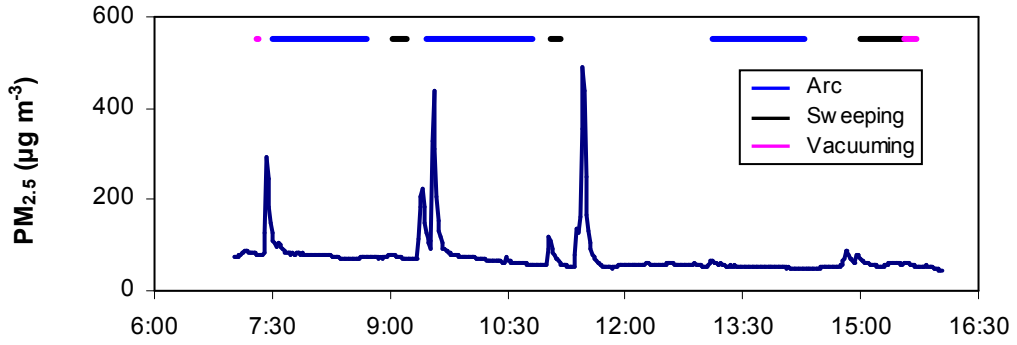

Figure 3.3. $PM_{2.5}$ time series at the background site inside the commercial plant on 25 July 2006, with the duration of production activities indicated by the bars across the top of the figure.

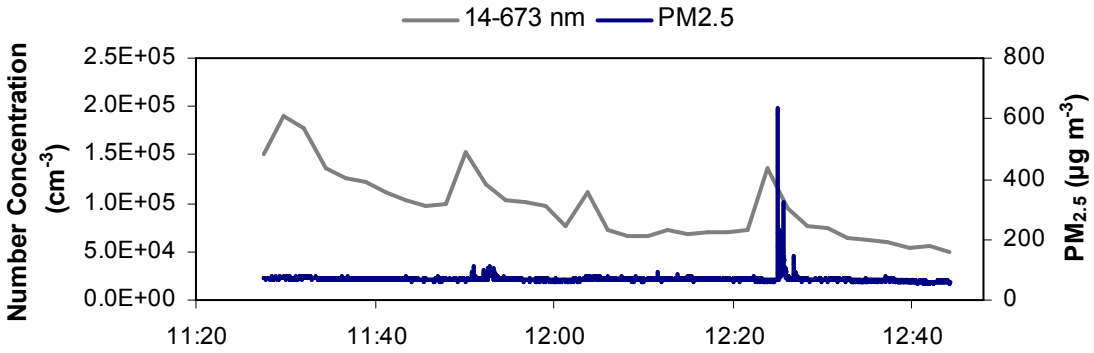

Figure 3.4. Particle number concentration and PM2.5 time series in ambient air outside the commercial plant on 25 July 2006.

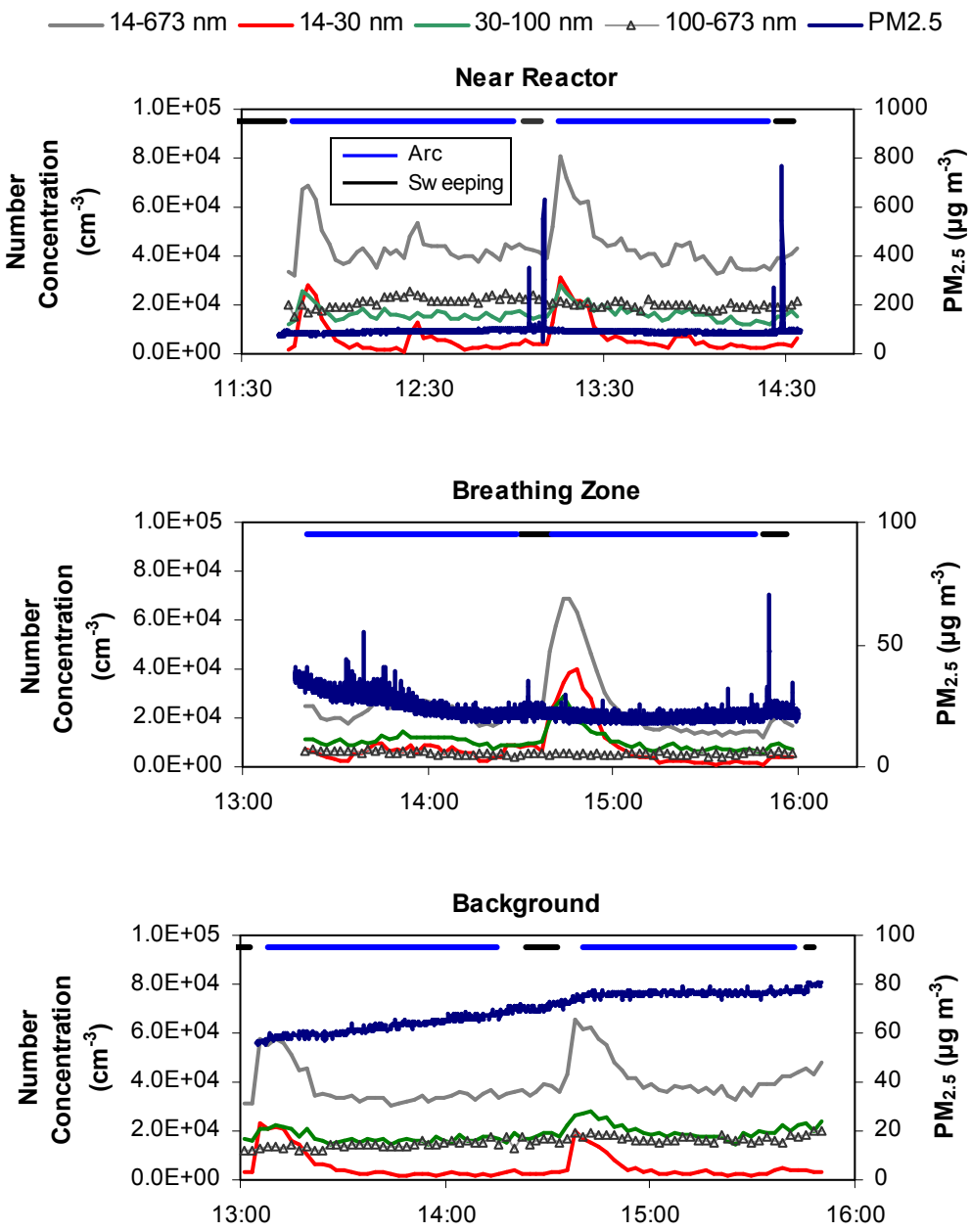

Figure 3.5. Particle number concentration and $PM_{2.5}$ time series in the university laboratory on 28 August 2006, with the duration of production activities indicated by the bars across the top of each panel. Number concentrations are shown as the total between 14-673 nm and as subsets of this range.

In the university laboratory in 2006, at each of the three locations we monitored two complete, successive production runs consisting of arc reaction and sweeping (Figure 3.5). We observed large spikes in $PM_{2.5}$, up to 700 µg m^{-3} above the baseline, near the reactor; smaller spikes of ~50

μg m^{-3} above baseline in the breathing zone; and no $PM_{2.5}$ spikes in the background. Baseline $PM_{2.5}$ concentrations were higher in the background than in the breathing zone, and $PM_{2.5}$ drifted upward during the four hours of sampling at the background location. Sweeping was typically accompanied by increases in $PM_{2.5}$ and/or particle number in all three locations, and the rises in number concentration lagged those in $PM_{2.5}$. At the background site, particle number concentrations but not $PM_{2.5}$ rose after sweeping. During sampling in the breathing zone, $PM_{2.5}$ was measured simultaneously at a second background location outside the reactor room. The average $PM_{2.5}$ concentration at this location was 26.6± 5.4 μg m^{-3}, similar to what was measured in the breathing zone.

Table 3.1 and Table 3.2 summarize $PM_{2.5}$ and total number concentrations by activity and location, averaged across production runs, in the commercial plant and the university laboratory, respectively. The supplemental information includes tables showing the results from individual production runs by activity and location.

In the commercial plant, the highest $PM_{2.5}$ concentrations occurred *near the reactor* during vacuuming. The average number of particles remained relatively unchanged throughout arcing and sweeping in the *background* location. However, $PM_{2.5}$ was higher during sweeping versus arc reaction in both the *near reactor* and *breathing zone* locations. Median particle diameters were 44-111 nm and were larger in the *background* compared to the other locations. In the university laboratory, $PM_{2.5}$ concentrations were more consistent across activities in any given location. Particle number concentrations were similar across all locations and activities. Here, median particle diameters ranged between 57-88 nm.

Table 3.1. Average $PM_{2.5}$ and particle number (14-673 nm) statistics across production runs in the commercial manufacturing plant in 2006.

	Near Reactor			Breathing Zone			Background		
	arc	**sweep**	**vacuum**	**arc**	**sweep**	**vacuum**	**arc**	**sweep**	**vacuum**
$PM_{2.5}$ ($\mu g\ m^{-3}$)									
Average	67.2	71.3	85.1	71.7	57.8	NA	73.0	57.1	53.3
Standard deviation	17.8	23.1	3.3	42.0	14.6	NA	53.9	6.2	6.2
Number of measurements[a]	8,152	882	60	8,539	1,039	NA	10,100	3,086	1,193
Runs	2	2	1	2	2	NA	2	2	2
Total number concentration (cm^{-3})									
Average	87,411	111,228	95,964	52,439	72,723	NA	52,735	51,063	33,066
Standard deviation	37,337	64,791	NA	6,537	6,890	NA	37,217	36,101	2,265
Total number of scans	93	6	1	33	9	NA	80	25	10
Runs	2	2	1	2	2	NA	2	3	2
Median diameter (nm)	53.3	43.7	47.8	50.5	75.1	NA	79.1	66.1	111

[a]Total number of measurements across all runs at 1-s intervals. The average and standard deviation are reported for this number of data points.

Table 3.2. Average $PM_{2.5}$ and particle number (14-673 nm) statistics across production runs in the university laboratory in 2006. $PM_{2.5}$ measurement at the background location was performed every 10-s.

	Near Reactor			Breathing Zone			Background		
	arc	**sweep**	**vacuum**	**arc**	**sweep**	**vacuum**	**arc**	**sweep**	**vacuum**
$PM_{2.5}$ ($\mu g\ m^{-3}$)									
Average	82.6	83.7	83.6	41.7	38.8	NA	54.5	54.9	NA
Standard deviation	10.4	26.0	28.5	17.9	17.8	NA	14.5	14.5	NA
Number of measurements[a]	16,535	1,984	451	20,484	2,338	NA	2,011	220	NA
Runs	4	4	1	5	5	NA	5	5	NA
Total number concentration (cm^{-3})									
Average	49,902	44,203	NA	45,685	26,898	NA	39,068	38,310	NA
Standard deviation	11,395	10,947	NA	16,888	10,803	NA	11,221	10,091	NA
Total number of scans	123	17	NA	121	17	NA	150	17	NA
Runs	4	4	NA	4	4	NA	5	5	NA
Median diameter (nm)	76.4	88.2	NA	57.3	82	NA	70	63.8	NA

[a]Total number of measurements across all runs at 1-s intervals in the *near reactor* and *breathing zone* locations and at 10-s intervals in the *background*. The average and standard deviation are reported for this number of data points.

Particle size distributions. Figure 3.6 shows size distributions of particles in the range 4-160 nm, measured using the NDMA during sweeping at three different locations in the commercial manufacturing facility in August 2005. Each solid line shows the average of 11 individual SMPS scans. The size distributions had a similar shape, with number concentration increasing with particle size. As shown in the supplemental information, the total number concentration was highest near the reactor with an average of 5,352±832 cm^{-3}; of medium value in the breathing zone, 4,834±925 cm^{-3}; and lowest in the background, 3,667±1311 cm^{-3}. Concentrations of the smallest particles, those less than 10 nm, were higher near the reactor (146±154 cm^{-3}) than in the breathing zone (79±130 cm^{-3}) and background (65±97 cm^{-3}), but there was large variability in their counts.

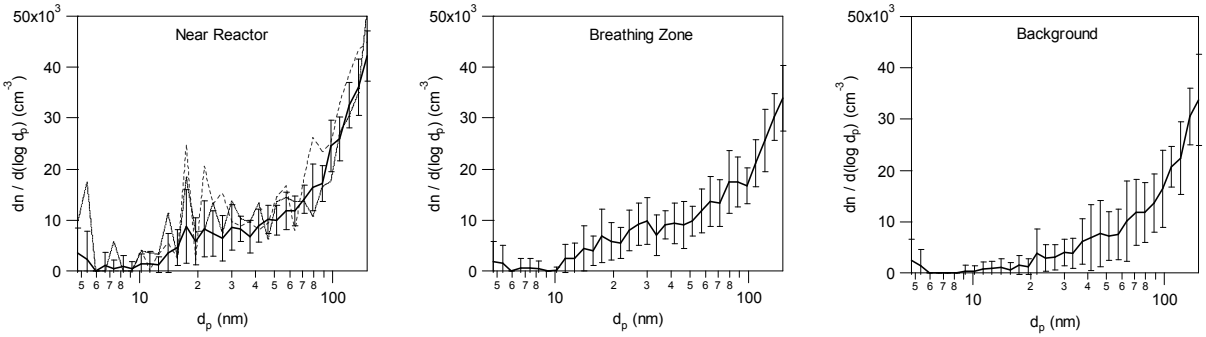

Figure 3.6. Average and standard deviation of nanoparticle size distributions at the commercial manufacturing facility during sweeping on 4 August 2005. The leftmost panel also includes two individual SMPS scans that show significantly enhanced concentrations around 5 and 20 nm

Because each SMPS scan takes 120 s, shorter periods of elevated number concentrations are captured only if the instrument happens to be dwelling on the relevant size at that time. In the near reactor case, two individual scans are indicated by the dotted and dashed lines, during which number concentrations were significantly enhanced around 5 or 20 nm. The additional resolution gained for particles smaller than 14 nm with the NDMA (4-160 nm) versus the LDMA (14-673

nm) did not appear to make up for the loss of information at larger sizes, so we used the LDMA for the remaining studies. The fraction of sub-160 nm particles smaller than 14 nm was 3-5% on average.

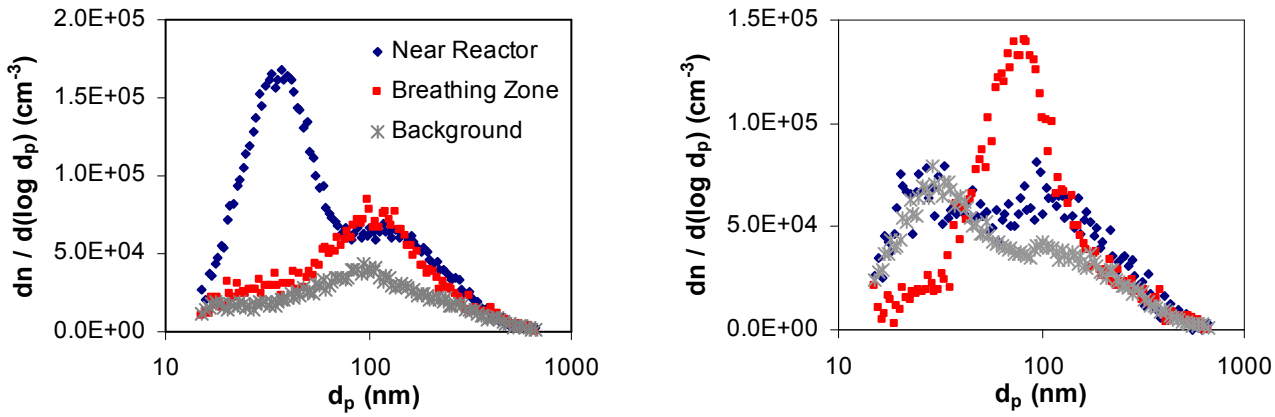

Figure 3.7. Particle size distributions at three locations in the commercial plant during arc reaction (a) and sweeping (b) on 25 July 2006.

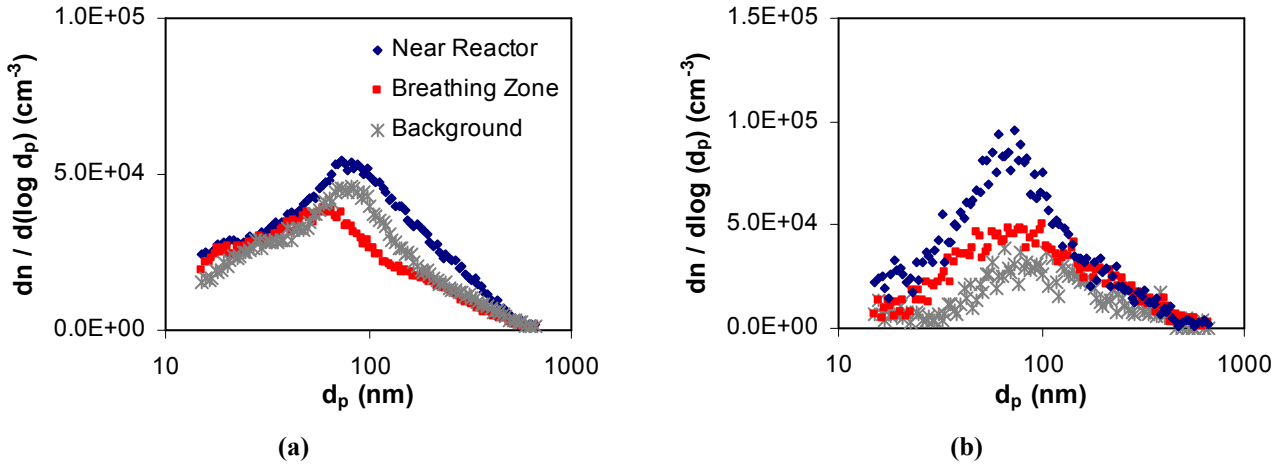

Figure 3.8. Submicron particle size distributions at three locations in the university laboratory during arc reaction (a) and sweeping (b) on 28-30 August 2006.

Figure 3.7 and Figure 3.8 illustrate size distributions of particles (14-673 nm) during arc reaction and sweeping at three different locations in both manufacturing facilities in 2006. In the

commercial manufacturing facility, the size distribution was bimodal near the reactor during arc reaction and unimodal at the other two locations. Near the reactor, modes occurred at ~30 and ~100 nm, while in the breathing zone and background, a single mode occurred at ~100 nm (Figure 3.7a). However, during sweeping, the size distributions were bimodal near the reactor and in the background and unimodal around ~90 nm in the breathing zone (Figure 3.7b). In contrast, Figure 3.8a shows that size distributions were very similar in magnitude and shape at different locations in the university laboratory during the arcing process, with modes at 80-90 nm. During sweeping, particle numbers in the range of 30-100 nm were enhanced near the reactor (Figure 3.8b). In all three locations at both manufacturing facilities, the mode of the size distributions fell in the nanoscale range, below 100 nm, during the sweeping of the reactors, as denoted in Table 3.1 and Table 3.2.

3.5 DISCUSSION

Particles are aerosolized during physical handling. Measurements clearly indicate that physical handling of the material results in the aerosolization of nanoparticles. Figure 3.2 and Figure 3.5 show that significant increases in sub-100 nm particle number concentrations are associated with vacuuming near the reactor in the commercial plant and with sweeping in all locations in the university laboratory. Table 3.1 also shows that the total number concentration is enhanced and that the median particle size is smaller during sweeping versus arc reaction and vacuuming at the commercial plant. Particle size distributions near the reactor during arc reaction are significantly enhanced around 30 nm compared to other locations (Figure 3.7). It is unclear if these particles remain suspended from previous activities or if something about the arc reaction produces them. The reactor is under vacuum, and particles should not be able to escape from it.

Larger particles are also suspended near the reactor during sweeping at the commercial plant, as indicated by the higher average $PM_{2.5}$ during this activity in Figure 3.1 and the spike in $PM_{2.5}$ at ~9:10, associated with sweeping, in the top panel of Figure 3.2. However, in this case, the total number concentration of sub-673 nm particles does not increase simultaneously. The relatively larger standard deviations in $PM_{2.5}$ near the reactor during sweeping as shown in Figure 3.1 also reflect the occurrence of large spikes in concentrations. In 2005, the maximum observed concentrations were 468 $\mu g\ m^{-3}$ on the first day and 1,569 $\mu g\ m^{-3}$ on the second day. Individual technique is likely to influence the measurements, as a different technician with a noticeably rougher touch performed the activities on the second day. In 2006, the maxima near the reactor were 2,443 $\mu g\ m^{-3}$ on the first day and 2,728 $\mu g\ m^{-3}$ on the second day.

Particles are also suspended in the breathing zone immediately before sweeping at the commercial plant (middle panel of Figure 3.2). Increases in both 100-673 nm particles and in $PM_{2.5}$ are observed, and the size distribution during sweeping is shifted with a mode near 90 nm (Figure 3.7). These particles may be associated with the technicians' physical activities in front of the fume hood in preparation for sweeping, i.e. rolling up a felt cloth covering the fume hood's shield, placing tools inside the fume hood, and opening the reactor. Human activities have been shown to increase exposure to PM through resuspension of dust (Adgate et al. 2002; Ferro et al. 2004; Liu et al. 2003).

Background particle concentrations may also influenced by nanomaterial production activities. As illustrated in Figure 3.3, sharp increases in $PM_{2.5}$ in the background are apparent shortly after sweeping or vacuuming in the commercial plant. Increases in both particle number and $PM_{2.5}$ are

evident before sweeping in the lower panel of Figure 3.2 and are probably related to activities in preparation for sweeping. The average total number concentration of particles decreases as the sampling location moves further away from reactor to the breathing zone and background locations, suggesting that activities surrounding the reactor are the source of airborne particles. At the university laboratory, increases in background particle number, but not $PM_{2.5}$, follow sweeping events (lower panel of Figure 3.5). The delayed timing after sweeping suggests that nanoparticles are being transported throughout the enclosure and eventually reach the background site. As shown in Table 3.2, the average $PM_{2.5}$ and total number concentrations were lower in the breathing zone as compared to near the reactor, but they were actually higher in the background than in the breathing zone during the sweeping period. Complex flow patterns introduced by a vacuum duct hanging above the reactor in the university laboratory may dilute concentration of particles in the breathing zone during sweeping, but application of a computational fluid dynamics model would be needed to confirm this hypothesis.

The slower decay in particle number concentrations compared to $PM_{2.5}$ (Figure 3.2 and Figure 3.5) likely results from the differing removal processes for larger versus smaller particles. The longer averaging time of the SMPS versus the DustTrak also plays a role but cannot entirely explain the pattern. In general, sweeping and vacuuming result in brief increases in larger particles and longer-lived increases in particles smaller than 100 nm. This is probably because the DustTrak is responding mainly to larger particles that settle out by gravity more quickly, while it is not as sensitive to smaller particles, whose mass is much less significant. At the same time, gravitational settling is less effective for smaller particles. Therefore, elevated

concentrations of submicron particles persist, while $PM_{2.5}$ concentrations return more rapidly to their baseline values.

The aerosolization of submicron particles in the workplace is not limited to nanotechnology facilities. Brouwer et al. (2004), for example, observed an increase in the number concentration of particles smaller than 750 nm generated from welding machines during and shortly after welding activities. However, in contrast to Maynard et al. (2004), who found no detectable release of nanoparticles associated with the handling of SWCNT, the results of the current study illustrate an increase in both $PM_{2.5}$ and sub-100 nm number concentration as a result of handling. Different control methods influence particle concentrations. Differences in particle concentrations between the commercial plant and the university laboratory probably reflect the use of different control methods in each facility. As noted in Table 3.1 and Table 3.2, total number concentrations of particles differ across locations and manufacturing steps in the commercial manufacturing facility but not in the university laboratory. The fume hood encasing each reactor at the commercial plant is probably more effective at removing nanoparticles suspended during sweeping than is the large, lower-flow-rate vacuum duct hanging above the reactor in the university lab. While an increase in airborne particle concentrations in the breathing zone occurs before sweeping at the commercial plant, such increases always lag sweeping in all locations of the university lab. This result suggests that the elevated levels of activity by workers in the commercial plant in preparation for sweeping contribute to the resuspension of particles. We observed that less movement occurs before sweeping in the university lab. The increases in particle number observed after sweeping in the breathing zone and background of the university lab suggest that nanoparticles are transported throughout the

large acrylic enclosure. Such behavior does not occur at the commercial plant. One similarity between the two facilities is that the median particle size is below 111 nm in all cases (Table 3.1 and Table 3.2), indicating that nanoscale particles are present at all times.

Ambient and background concentrations are important. Outdoor ambient concentrations of airborne particles appear to influence the measurements. Figure 3.1 shows that all concentrations are higher on the first day (4 August) compared to the second (9 August) in the commercial facility in 2005, probably reflecting differences in ambient concentrations on the two days. The nearest ambient $PM_{2.5}$ monitoring site is located 100 km away. Filter samples (24-h) are collected every three days at this location, and 4 August fell in between the some of the highest measurements of the year: 35 μg m^{-3} on 2 August and 37 μg m^{-3} on 5 August. By 8 August, 24-hr $PM_{2.5}$ had dropped to 16 μg m^{-3}. Not only daily, but also hourly variations in ambient PM concentrations may influence the measurements, as small particles easily penetrate from outdoors to indoors (Bennett and Koutrakis 2006; Hovorka et al. 2005; Zhu et al. 2005). The variations in baseline $PM_{2.5}$ at different locations (Figure 3.2 and Figure 3.5) may reflect diurnal changes in ambient particle concentrations because these measurements took place at different times of day.

Even over a period of just 80 minutes, measurements outside the commercial plant show considerable variability in number concentrations and $PM_{2.5}$ (Figure 3.4). Particle number concentrations generally decrease over the period, with four small spikes lasting a few minutes at most. $PM_{2.5}$ hovers around 68 μg m^{-3}, except for a sudden increase lasting ~60 s to a maximum of 635 μg m^{-3}, probably due to the arrival of a vehicle in the gravel and dirt parking lot. In future

studies, it will be important to control for changes in background ambient particle concentrations by either isolating the study area from such influence, as done by Maynard et al. (2004) with a tent, or by conducting simultaneous background measurements during all experiments.

Size distributions also exhibit day-to-day differences. Portions of the size distributions measured in the commercial plant with the NDMA versus the LDMA overlap between 14-160 nm. While Figure 3.6 shows only slight differences in 4-160 nm number concentrations across locations, Figure 3.7 shows that on another day, differences are significant for sub-160 nm particles. Differences across production runs (time of day) may reflect the presence of other particle sources in the room, such as drilling and personal dust resuspension, changes in ventilation of the room, and/or changes in ambient concentrations throughout the day. Due to equipment limitations, we sampled at each location in series and were not able to obtain simultaneous measurements in multiple locations except for continuous background measurements in the commercial plant on one day.

The sampling techniques used in this study do not differentiate between particles generated by nanomaterial soot production and those from other sources. To overcome this limitation, further investigation is needed that includes chemical analysis to facilitate source apportionment of airborne particles. Additionally, faster scanning methods for measuring particle size distributions will enable more reliable detection of short-lived concentration peaks.

3.6 CONCLUSION

We have investigated the potential risk of exposure to airborne particles in two nanomaterials manufacturing facilities, a commercial plant and a university laboratory. Physical handling of the material, either by sweeping or vacuuming, results in elevated concentrations of $PM_{2.5}$ and particle number. In both facilities, the increase in total number concentration of particles (14-673 nm) can be attributed mainly to an increase in the number of particles smaller than 100 nm, so nanoparticles are clearly suspended during such activities. Physical movements by the workers results in the suspension of larger particles. As expected, containment of the reactor inside a fume hood limits the spreading of nanoparticles throughout the facility. This study contributes important new data regarding exposure to engineered nanoparticles. However, results from other facilities and other types of nanomaterials are needed to support the development of guidelines and regulations to protect human health and the environment. Additionally, such studies need to account for variations in ambient and background particles and to be able to distinguish between the nanomaterial of interest versus other airborne particles.

3.7 ACKNOWLEDGMENTS

This work was supported by a Virginia Tech ASPIRES grant, the National Science Foundation (BES-0537117), and a Sussman Foundation fellowship to B. Yeganeh. We also thank Luna NanoWorks for access to its facility and Carolyn Stevens of the Virginia Department of Environmental Quality for providing ambient air monitoring data.

3.8 REFERENCES

Adgate, J. L., Ramachandran, G., Pratt, G. C., Walker, L. A., and Sexton, K. (2002). "Spatial and temporal variability in outdoor, indoor and personal $PM_{2.5}$ exposure." *Atmospheric Environment*, 36, 11.

Aitken, R. J., Chaudhry, M. Q., Boxall, A. B. A., and Hull, M. (2006). "Manufacture and use of nanomaterials: current status in the UK and global trends." *Occupational Medicine-Oxford*, 56(5), 300-306.

Bennett, D. H., and Koutrakis, P. (2006). "Determining the infiltration of outdoor particles in the indoor environment using a dynamic model." *Journal of Aerosol Science*, 37(6), 20.

Borm, P. J. A. (2002). "Particle toxicology: from coal mining to nanotechnology." *Inhalation Toxicology*, 14, 14.

Borm, P. J. A., and Kreyling, W. (2004). "Toxicological hazards of inhaled nanoparticles-potential implications for drug delivery." *Journal of Nanoscience and Nanotechnology*, 4, 11.

Brouwer, D. H., Gijsbers, J. H. J., and Lurvink, M. W. M. (2004). "Personal exposure to ultrafine particles in the workplace: Exploring sampling techniques and strategies." *Annals of Occupational Hygiene*, 48(5), 439-453.

Colvin, V. L. (2003). "The potential environmental impact of engineered nanomaterials." *nature Biotechnology*, 21, 5.

Dhawan, A., Taurozzi, J. S., Pandey, A. K., Shan, W. Q., Miller, S. M., Hashsham, S. A., and Tarabara, V. V. (2006). "Stable colloidal dispersions of C-60 fullerenes in water: Evidence for genotoxicity." *Environmental Science & Technology*, 40(23), 7394-7401.

Donaldson, K., Li, X. Y., and MacNee, W. (1998). "Ultrafine (nanometre) particle mediated lung injury." *Journal of Aerosol Science*, 29(5-6), 553-560.

Donaldson, K., Stone, V., Gilmour, P. S., Brown, D. M., and MacNee, W. (2000). "Ultrafine particles: mechanisms of lung injury." *Philosophical Transactions of the Royal Society of London Series a-Mathematical Physical and Engineering Sciences*, 358(1775), 2741-2748.

Ferro, A., Kopperud, R. J., and Hildemann, L. M. (2004). "Elevated personal exposure to particulate matter from human activities in a residence." *Journal of Exposure Analysis and Environmental Epidemiology*, 14, 7.

Fortner, J. D., Lyon, D. Y., Sayes, C. M., Boyd, A. M., Falkner, J. C., Hotze, E. M., Alemany, L. B., Tao, Y. J., Guo, W., Ausman, K. D., Colvin, V. L., and Hughes, J. B. (2005). "C-60 in water: Nanocrystal formation and microbial response." *Environmental Science & Technology*, 39(11), 4307-4316.

Gwinn, M. R., and Vallyathan, V. (2006). "Nanoparticles: Health effects - Pros and cons." *Environmental Health Perspectives*, 114(12), 1818-1825.

Hovorka, J., Holub, R. F., Branis, M., and Honeyman, B. D. (2005). "Tracing outdoor/indoor penetration of PM2.5, PM1.0 by Po-210/Pb-210." *Indoor and Built Environment*, 14(3-4), 5.

Jia, G., Wang, H. F., Yan, L., Wang, X., Pei, R. J., Yan, T., Zhao, Y. L., and Guo, X. B. (2005). "Cytotoxicity of carbon nanomaterials: Single-wall nanotube, multi-wall nanotube, and fullerene." *Environmental Science & Technology*, 39(5), 1378-1383.

Lam, C. W., James, J. T., McCluske, R., and Hunter, R. L. (2004). "Pulmonary toxicity of single-wall carbon nanotubes in mice 7 and 90 days after intratracheal instillation." *Toxicological Sciences*, 77, 9.

Liu, L. J. S., Box, M., Kalman, D., Kaufman, J., Koenig, J., Larson, T., Lumley, T., Sheppard, L., and Wallace, L. (2003). "Exposure assessment of particulate matter for susceptible population in Seattle." *Environmental Health Perspectives*, 111, 10.

Maynard, A. D., Baron, P. A., Foley, M., Shvedova, A. A., Kisin, E. R., and Castranova, V. (2004). "Exposure to carbon nanotube material: Aerosol release during the handling of unrefined single-walled carbon nanotube material." *Journal of Toxicology and Environmental Health-Part A*, 67(1), 87-107.

Maynard, A. D., and Kuempel, E. D. (2005). "Airborne nanostructured particles and occupational health." *Journal of Nanoparticle Research*, 7(6), 587-614.

Oberdörster, E. (2004). "Manufactured nanomaterials (Fullerenes, C-60) induce oxidative stress in the brain of juvenile largemouth bass." *Environmental Health Perspectives*, 112(10), 1058-1062.

Oberdörster, G. (2001). "Pulmonary effects of inhaled ultrafine particles." *International Archives of Occupational and Environmental Health*, 74(1), 1-8.

Oberdörster, G., Oberdörster, E., and Oberdörster, J. (2005). "Nanotoxicology: An emerging discipline evolving from studies of ultrafine particles." *Environmental Health Perspectives*, 113(7), 823-839.

Peters, A., Wichmann, E., Tuch, T., Heinrich, J., and Heyder, J. (1997). "Respiratory effects are associated with the number of ultrafine particles." *American Journal of Respiratory and Critical Care Medicine*, 155, 18.

Pope, C. A., Burnett, R. T., Thun, M. J., Calle, E. E., Krewski, D., Ito, K., and Thurston, G. D. (2002). "Lung cancer, cardiopulmonary mortality, and long-term, exposure to fine particulate air pollution." *Journal of the American Medical Association*, 287, 10.

Roco, M. C. (2005). "Environmentally responsible development of nanotechnology." *Environmental Science & Technology*, 39(5), 106A-112A.

Stevenson, S., Rice, G., Glass, T., Harich, K., Cromer, F., Jordan, M. R., Craft, J., Hadju, E., Bible, R., Olmstead, M. M., Maitra, K., Fisher, A. J., Balch, A. L., and Dorn, H. C. (1999). "Small-bandgap endohedral metallofullerenes in high yield and purity." *Nature*, 401, 55-57.

Tsuji, J. S., Maynard, A. D., Howard, P. C., James, J. T., Lam, C. W., Warheit, D. B., and Santamaria, A. B. (2006). "Research strategies for safety evaluation of nanomaterials, part IV: Risk assessment of nanoparticles." *Toxicological Sciences*, 89(1), 42-50.

van Poppel, L. H., Friedrich, H., Spinsby, J., Chung, S. H., Seinfeld, J. H., and Buseck, P. R. (2005). "Electron tomography of nanoparticle clusters: Implications for atmospheric lifetimes and radiative forcing of soot." *Geophysical Research Letters*, 32 Art. No. L24811.

Warheit, D. B., Laurence, B. R., Reed, K. L., Roach, D. H., Reynolds, G. A. M., and Webb, T. R. (2004). "Comparative pulmonary toxicity assessment of single-wall carbon nanotubes in rats." *Toxicological Sciences*, 77(9), 117.

Wiesner, M. R., Lowry, G. V., Alvarez, P., Dionysiou, D., and Biswas, P. (2006). "Assessing the risks of manufactured nanomaterials." *Environmental Science & Technology*, 40(14), 4336-4345.

Zhu, Y. F., Hinds, W. C., Krudysz, M., Kuhn, T., Froines, J., and Sioutas, C. (2005). "Penetration of freeway ultrafine particles into indoor environments." *Journal of Aerosol Science*, 36(3), 20.

.

CHAPTER 4

AEROSOLIZATION OF C_{60} FULLERENE AND THEIR COLLECTION IN WATER USING AN IMPINGER

4.1 ABSTRACT

Despite the rapid growth in nanotechnology, very little is known about the properties of manufactured nanomaterials in the atmosphere. To facilitate life cycle assessments of nanomaterials in the atmosphere, reliable and repeatable methods are needed to generate aerosolized engineered nanoparticles. We have used an atomizer to aerosolize C_{60} aggregates from a fullerene-water suspension that was prepared through extended stirring. Measurement of particle size distributions and number concentrations shows that increasing the initial aqueous-phase fullerene concentration results in an increase in the number concentration of aerosolized particles, while the average size of particles remains relatively constant and unimodal at ~40 nm. To return the aerosolized fullerenes back into water, we passed the aerosol sample through a liquid impinger. Decreasing the flow rate through the impinger results in significantly increased collection efficiency of sub-100 nm particles. Extending the stirring period during preparation of the fullerene-water suspensions also results in an increase in the collection efficiency of airborne nanoparticles, up to 99%.

4.2 INTRODUCTION

Nanoparticles are typically defined as particles with one dimension of less than 100 nm. The unique properties of these materials are being exploited in a growing number of applications (Gwinn and Vallyathan 2006), which are expected to revolutionize products and grow to a market of $1 trillion by 2015 (Roco 2005). Given the rapid growth in nanotechnology, more studies are needed on the health and environmental effects of engineered nanomaterials.

Health and environmental risk assessments and life-cycle analyses of nanomaterial-based products require an improved understanding of the nature of nanomaterials in aquatic, atmospheric, and terrestrial environments (Wiesner et al. 2006). Several recent studies have suggested that manufactured nanomaterials may have significant deleterious effects on health. Carbon nanotubes showed evidence of toxicity to mice, rats, and eukaryotic cells, compared to equivalent doses of quartz, which itself is considered a serious occupational health hazard (Jia et al. 2005; Lam et al. 2004; Warheit et al. 2004). Oberdörster (2004) reported that manufactured C_{60} fullerenes induced oxidative stress in the brains of fish, and Dhawan et al. (2006) showed that suspensions of C_{60} in water exhibited genotoxicity. Exposure to C_{60} also inhibited the growth and respiration rates of microbes (Fortner et al. 2005), although it demonstrated no toxic effects on eukaryotic cells (Jia et al. 2005).

Determining the risk presented by inhaled nanoparticles, however, requires toxicity studies in which test subjects are exposed to aerosolized particles. In the previously mentioned studies involving engineered nanoparticles, the nanoparticles were administered by intratracheal instillation or suspension in the liquid environment of the organisms but not by inhalation.

Definitive toxicity studies on the inhalation risk of nanoparticles will require that controlled amounts of aerosolized material be delivered to the test subjects' respiratory systems. One challenge presented by nanoparticles, because of their large surface area relative to mass, is their tendency to aggregate. The traditional method of administering powders for inhalation studies—mechanically dispersing the material into an air stream—does not provide sufficient force to deaggregate the particles into nanoscale sizes which are likely to be more relevant for engineered nanoparticles.

Controlled experiments involving aerosolized nanoparticles are also important for determining their environmental fate. The physical characteristics of nanomaterials in the atmosphere, such as size distribution, concentration, and tendency to aggregate and deposit, play a key role in determining their longevity in the natural environment. Research involving dispersion of C_{60} fullerenes in water has shown that they have low affinities for the aqueous phase (McHedlov-Petrossyan et al. 1997), form relatively large aggregates with a mean diameter >170 nm (Alargova et al. 2001; Brant et al. 2005a; Brant et al. 2005b; Brant et al. 2006; Dhawan et al. 2006), and produce relatively stable amber-colored aqueous suspensions at very low ionic strengths (Andrievsky et al. 1995; Brant et al. 2005b; Brant et al. 2005c). There is a direct correlation between the behavior of particles in suspension and their size, structure, and chemical characteristics (Weibel et al. 2005). However, the physical characteristics of nanoparticles in aerosolized form, as well as the transport of nanomaterials between liquid and gaseous phases, have received less attention. These shortcomings call for further research involving airborne nanomaterials: studies on their fate and transport in the atmosphere and their inhalation toxicology.

Furthermore, it may be advantageous to transfer airborne nanoparticles to liquid to facilitate chemical analysis (e.g. high-pressure liquid chromatography, spectrophotometry) and studies of cross-media effects of nanomaterials. This approach also represents a potential control technology for removing nanoparticles from a highly concentrated gaseous waste stream. The most commonly used apparatus for trapping airborne particles in water is the impinger, which is often employed for sampling bioaerosols. In an impinger, an air stream is forced through a liquid bath, and impaction of airborne particles into the liquid and the bottom surface of the liquid reservoir as bubbles form is usually considered to be the main collection mechanism (Grinshpun et al. 1997). Studies evaluating the collection efficiencies of impingers have focused on particles in the millimeter size range (Kim et al. 2002; Lin et al. 1997; Tseng and Li 2005; Willeke et al. 1998), while the collection efficiency of impingers for submicron particles has received less attention. In one such study, the collection efficiency for particles of diameter 20 nm was shown to be less than 20% (Spanne et al. 1999). Another study found a collection efficiency of less than 10% for particles in the 30-100 nm size range (Hogan et al. 2005), indicating the inadequacy of impingers for collecting nanoscale particles under the experimental conditions considered.

Previous studies suggest that the collection efficiencies in impingers are monotonically increasing functions of particle inertia, i.e. size and velocity, because of the importance of impaction as a collection mechanism. Therefore, an increase in flow rate through the sampler has been assumed to result in a collection efficiency that asymptotically approaches 100% for a given particle size (Grinshpun et al. 1997; Kim et al. 2002; Lin et al. 1997). However, this logic is only valid for larger particles. While impaction is ineffective for nanoscale particles, the main collection mechanism acting on them is diffusion through Brownian motion (Hogan et al. 2005),

which increases with decreasing particle size. For these types of particles, a lower flow rate will provide smaller bubbles and a longer residence time inside the liquid reservoir, allowing a shorter diffusion path length and more time for the particles to diffuse into the body of water. On the contrary, increasing the flow rate will eventually decrease the collection efficiency of nanoscale particles due to the larger bubble size and decrease in residence time within the sampler. Existing studies of impinger collection efficiencies, however, have not considered flow rates of less than 0.7 L min^{-1}.

The goals of this research are to generate aerosolized nanoparticles from an aqueous solution in a controlled manner, to characterize their properties, and to quantify their collection efficiency back into water in an impinger. We are considering C_{60} fullerenes as our model nanoparticle because they are already being produced commercially in large quantities and because few studies of their atmospheric properties exist. To fulfill the research objectives, we measure size distributions and number concentrations of airborne particles generated from aqueous-phase fullerene samples with varying initial concentrations. We then use an impinger to collect airborne particles in water and calculate its collection efficiency for removing nanoparticles with diameters less than 100 nm.

4.3 MATERIALS AND METHODS

4.3.1 Sample Preparation

Suspensions of C_{60} fullerenes (Sigma Aldrich, Saint Luis, MO) were prepared through extended mixing in water (Brant et al. 2005a; Brant et al. 2005b; Brant et al. 2006; Dhawan et al. 2006).

The extended mixing of powdered C_{60} in water, rather than preparation using intermediate solvents such as tetrahydrofuran, is of special importance as it corresponds more closely to natural environmental transport scenarios (Dhawan et al. 2006). We stirred powdered fullerene in water over a period of time, usually two weeks, with a magnetic stirrer at 600 rpm. Henceforth, we refer to the fullerene-water suspension as nC_{60}, where n represents some number of molecules that form fullerene aggregates. For the first part of the research—the *characterization* of aerosolized fullerene—four replicates of each sample with initial concentrations of 0.2, 0.4, and 0.8 mg mL^{-1} were prepared. For the second part—measurement of the *collection* efficiency of airborne fullerene nanoparticles in an impinger—three samples with three replicates of each were prepared. Two sets of samples with initial concentrations of 0.4 and 0.8 mg mL^{-1} were stirred for 2 weeks, while the third set with a concentration of 0.8 mg mL^{-1} was stirred for more than 4 months. Figure 4.1 illustrates the changes in the color of nC_{60} fullerene suspensions over time.

(a) **(b)**

Figure 4.1. Changes in the color of nC_{60} samples as the stirring period progresses: a) after 3 days, b) after 9 days.

The characterization study used water treated with a laboratory-based purification system (NANOpure, Apple Scientific, Chesterland, OH) and filtered through 0.22 µm PES filters (GP

Express Plus Membrane, Fisher Scientific, Hampton, NH). The collection study used water purchased from a supplier (Optima, Fisher Scientific). After stirring, we filtered the nC_{60} solution through 0.45 μm cellulose membrane filters (Fisher Scientific) to remove the larger aggregates. We used new traceable glassware for the preparation and storage of all samples and stored the solutions in amber glassware or in the dark at room temperature. All bottles and Teflon-coated stir bars were rinsed once with aqua regia (a mixture of one part by volume of concentrated nitric acid and three parts of concentrated hydrochloric acid), four times with laboratory purified water, and once with Optima water and were stored in a desiccator.

4.3.2 Experimental Setup

nC_{60} Characterization. The samples were aerosolized using a constant output atomizer (TSI 3076, Shoreview, MN), which generates a spray of particles by subjecting a thin liquid stream to a high-velocity jet of air. Large droplets impact onto the wall opposite the jet and drain out of the system, while smaller droplets remain suspended in air. In contrast to mechanical techniques of dispersing powders, this method produces much smaller aerosolized particles. We ran the atomizer in non-recirculation mode and injected the nC_{60} solution using a 100-mL all-glass syringe (Popper & Sons, Inc. 5177, New Hyde Park, NY) installed on a syringe pump (Harvard Apparatus PHD 2000, Plymouth Meeting, PA). The syringe pump insured a constant liquid flow to the atomizer at a rate of 0.59 mL min^{-1}. Since fresh liquid was supplied continually to the atomizing head by the syringe pump and the excess liquid collected by impaction was not recirculated back to the syringe pump, the system's performance was very stable.

The complete experimental setup is shown in Figure 4.2., which depicts two routes, one used for

the characterization study and the other used for the collection study. For the characterization study, ultra zero-grade air at the rate of 1.75 L min^{-1} was used as the supply air into the system. Flow rates were controlled by mass flow controllers (EW-32907-71, Cole-Parmer, Vernon Hills, IL). The outflow from the atomizer was diluted with ultra zero-grade air, also at a flow rate of 1.75 L min^{-1}, to partially dry the particles. The air stream then passed through a diffusion dryer (TSI 3062) to further dry the particles. Finally, the aerosol passed through a neutralizer (TSI 3077) that removed electrostatic charges from the particles. All tubing was either copper or conductive silicone.

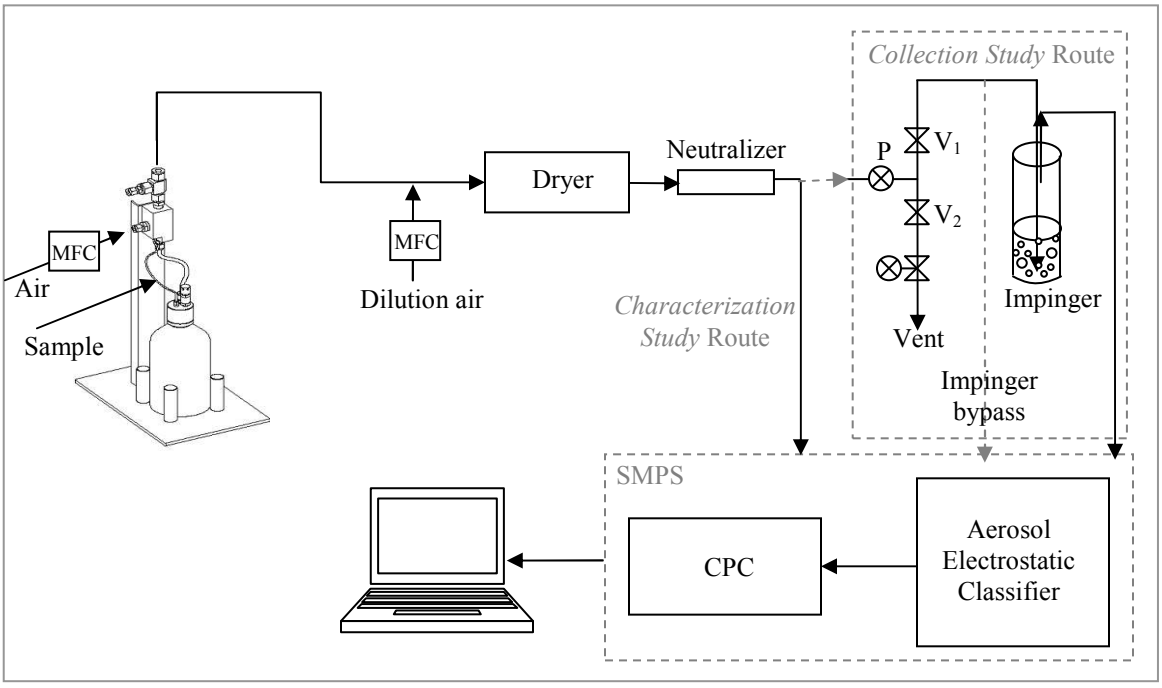

Figure 4.2. Experimental setup for nC_{60} characterization and collection efficiency studies.

Particle losses in the system were minimal. We calculated that 5 to 10% of particles would be lost due to diffusion to tubing surfaces (Seinfeld and Pandis 2006). We also calculated the rate of change in total number concentration of particles in air due to coagulation (Seinfeld and Pandis 2006). Over all combinations of particle sizes between 14.8 and 661 nm, the maximum loss was

estimated to be 2.9%, which was for the particles in the range of 14.8-20.55 nm. A humidity-temperature probe (hygroPalm1-HygroClip SC04, Rotronic, Huntington, NY) recorded relative humidity and temperature inside the tubing.

In addition to testing each replicate separately, we also combined all the replicates of a single concentration in equal volumes and performed an additional set of measurements using this blended sample. Before each experiment, we ran a control consisting of laboratory purified and filtered water only. Even a miniscule amount of impurities, mainly salts, in the water can result in measurable concentrations of particles. We calculated the maximum volume concentration of aerosolized particles in our system, due to water residue alone, assuming a maximum residue concentration of 1 ppm in water, as specified for the Optima water, and a solids density of 1 g cm^{-3}. This value was significantly higher than the measured particle volume concentration from Optima water; therefore the residue in water can explain entirely the presence of particles when "pure" water is aerosolized.

Particle Measurement. Particle size distributions and number concentrations were measured in situ using a scanning mobility particle sizer (TSI SMPS 3936) equipped with a long differential mobility analyzer (LDMA) and an ultrafine condensation particle counter (TSI CPC 3025A). The differential mobility analyzer selects specific sizes of airborne particles based on electrical mobility, and the CPC exposes the particles to supersaturated conditions to grow them to large enough sizes that they can be detected by light scattering. We ran the instrument continuously in scanning mode over the range of particle diameters (d_p) 14-673 nm. Each scan takes 120 s, and the maximum detection limit is 10^7 particles cm^{-3}. For the purpose of this research, we averaged

the reported number concentrations in any particle size range across as many scans as were recorded during the measurement period. The SMPS's Aerosol Instrument Manager Software was used to control the sampling and counting process, as well as for data acquisition.

The instruments were calibrated using polystyrene latex spheres (PSL, Duke Scientific Corp., Fremont, CA) several times throughout the course of the experimental study, as shown in Figure 4.3. While the mode of each size distribution occurred near the nominal sphere size, measurements were strongly influenced by background impurities from the water.

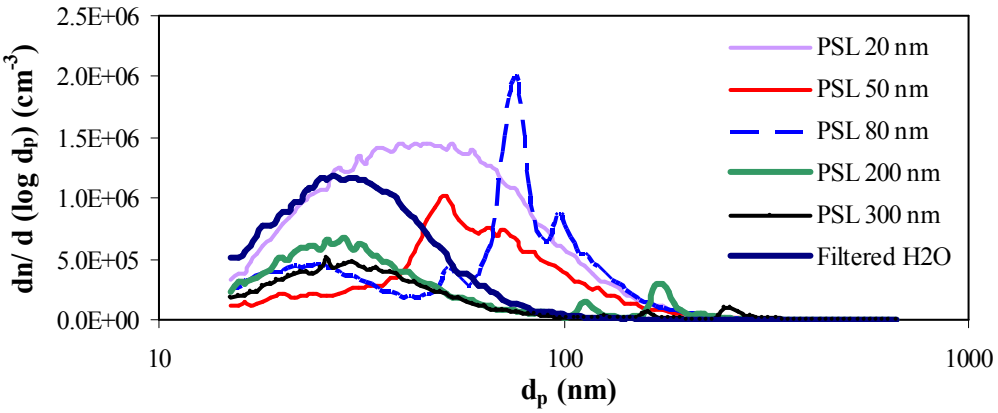

Figure 4.3. Size distributions of aerosolized PSLs measured by the SMPS.

nC_{60} Collection Efficiency. Aerosolized nC_{60} was collected in a glass impinger (AGI-4 ACE Glass, Vineland, NJ) (Figure 4.4.), containing 100 mL of Optima water, after neutralization and before entering the SMPS through the *collection study* route (Figure 4.2.). In this configuration, the presence of high physical resistance in the system caused unsteady injection of the sample from the syringe pump, so we instead operated the system in recirculation mode, with the liquid sample drawn from the atomizer's 1 L jar. In this case, we used ultra zero-grade air at flow rates of 2.0 L min^{-1} and 1.0 L min^{-1} for the supply and dilution air, respectively.

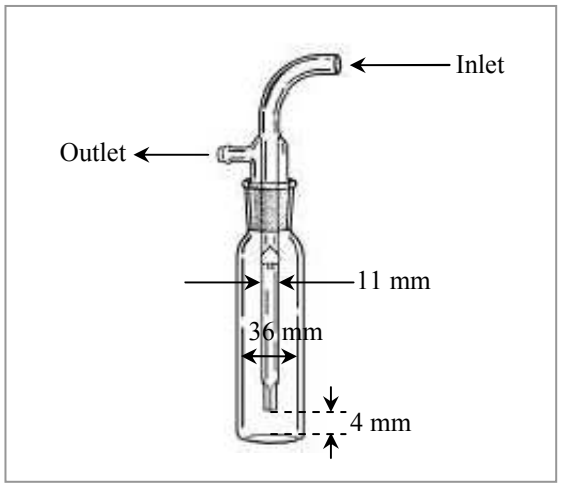

Figure 4.4. Dimensions of the impinger used in this study (AGI-4): capillary diameter = 1 mm, length of capillary = 20 mm, length of inlet tube = 164 mm, volume of flask = 125 mL, recommended airflow = 6 L min^{-1} (adapted from ACE-Glass website).

The flow to the particle analyzers was adjusted by slightly opening valve V_1 (Figure 4.2.), until the flow rate reached the SMPS's programmed set point of 0.1 L min^{-1}. The remaining air was vented through valve V_2, which was left totally open. We also investigated an alternative setup with a flow rate of 3.0 L min^{-1} through the impinger. The manufacturer recommended a flow rate of 6.0 L min^{-1}, but we found this rate to produce highly unstable results.

To test the collection efficiency of nC_{60} in water, we compared particle number concentrations measured after the impinger to those measured when the flow bypassed the impinger (dashed arrow in Figure 4.2.). We then calculated the collection efficiency η as

$$\eta = \frac{(C_{ref} - C_{imp})}{C_{ref}} \times 100$$

where C_{ref} is the number concentration of particles in flow that bypassed the impinger and C_{imp} is the number concentration of particles in flow that passed through the impinger.

Figure 4.5. compares the size of bubbles in the impinger with two different flow rates. The size of air bubbles was significantly smaller at a flow rate of 0.1 L min^{-1} versus 3.0 L min^{-1}. There were many very small bubbles (< 0.1 mm) in the water reservoir under the lower flow rate conditions, but these were not visible to the camera.

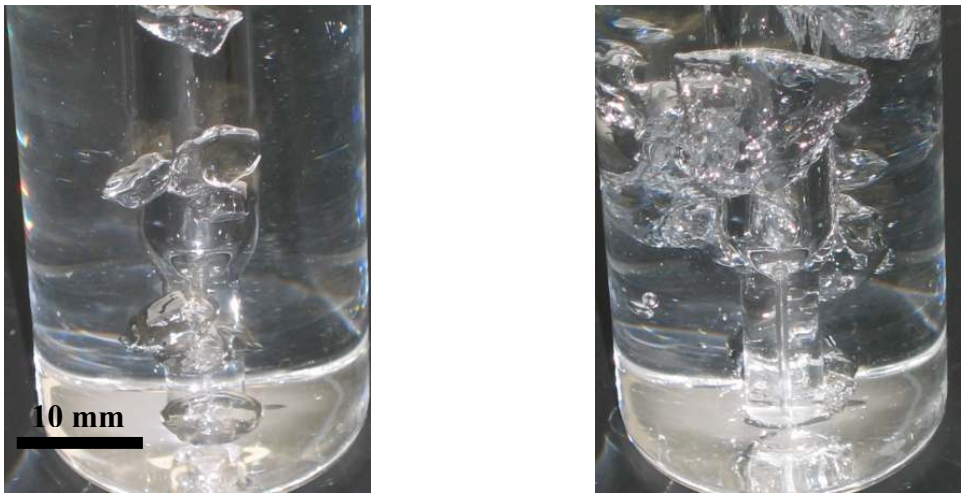

Figure 4.5. Shapes of bubbles rising in the column of water inside the impinger reservoir at flow rates of a) 0.1 L min^{-1}, b) 3 L min^{-1}.

To examine the particles' morphology and size in greater detail, we collected samples on grids for analysis by Transmission Electron Microscopy (TEM). We placed the grids inside the tubing during experimental runs for at least 30 min.

4.4 RESULTS

Figure 4.6. shows nC_{60} residuals after filtration through a 0.45 μm pore size filter. The residuals from the sample stirred for 2 weeks appear as bulky dark brown-black crystals, randomly clustered together on the surface, while the residuals from the samples stirred for 4 months result in a more uniform brownish layer on the filter media.

(a) **(b)**

Figure 4.6. Filtered C_{60} fullerene samples a) after 2 weeks, b) after 4 months.

4.4.1 Fullerene Aerosolization

Figure 4.7 shows normalized size distributions of aerosolized fullerenes for the combined sample. The size distributions averaged across the four replicates (not shown) are similar to that of the combined sample. As the figure illustrates, the number of aerosolized particles in the

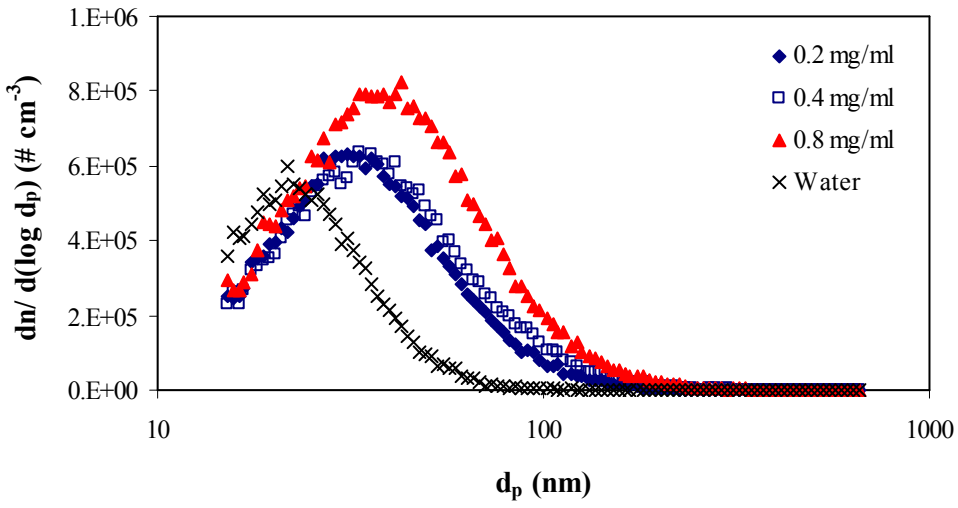

Figure 4.7. Normalized number concentration of aerosolized C_{60} fullerene particles.

samples with initial concentrations of 0.2 and 0.4 mg mL^{-1} are not significantly different, while the number of aerosolized particles is much higher for the sample with an initial concentration of 0.8 mg mL^{-1}. The size distributions have modes of 31.1, 33.4, and 42.9 nm for samples with initial concentration of 0.2, 0.4, and 0.8 mg mL^{-1}, respectively.

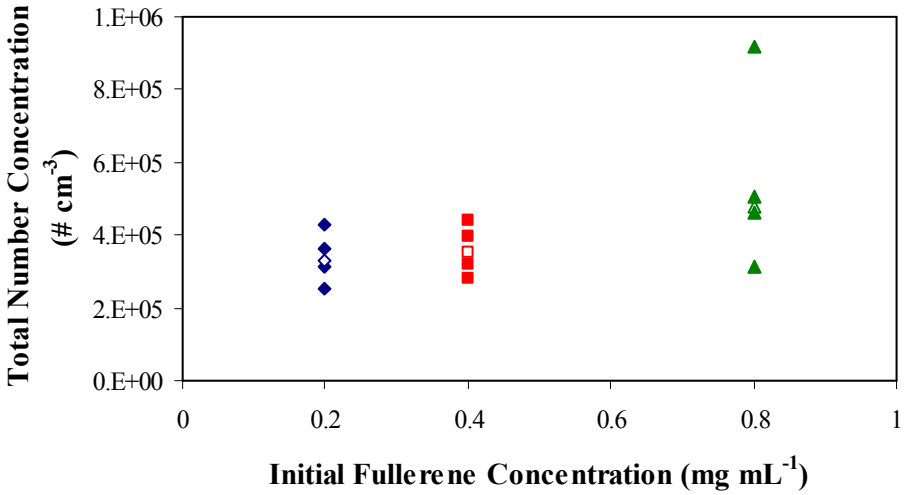

(a)

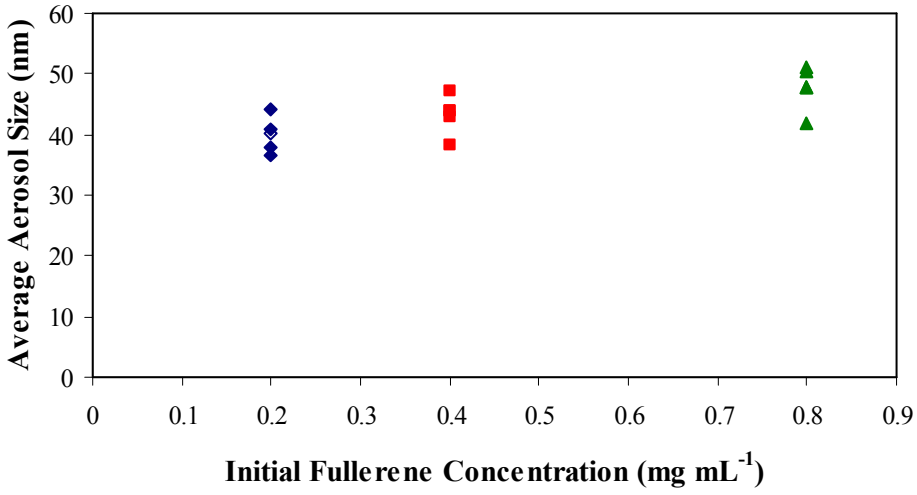

(b)

Figure 4.8. Physical characteristics of aerosolized nC_{60} fullerene aggregates as a function of initial aqueous-phase concentration: a) total number concentration, b) size. The solid symbols represent each of the sample replicates, while the open symbols represent the combined samples, a measured average.

Figure 4.8. presents the total number concentration and average size of particles as a function of initial aqueous-phase concentration. The solid symbols represent each of the replicates, while the open symbols represent the combined samples, a measured average. Although there is substantial scatter in the replicates, in general the total number concentration of particles increases with the initial concentration of fullerenes in water, but the relationship is not linear through the origin. The average size of aerosolized particles also increases slightly with the initial concentration of C_{60} in water; however, the differences are not significant. Table 4.1 presents the physical properties of aerosolized particles as a function of aqueous-phase concentration.

Table 4.1. Total number concentration and average size of nC_{60} fullerene aerosolized from aqueous suspensions of combined samples, a measured average, at three concentrations. Standard deviations are calculated across multiple scans.

	Initial Aqueous-Phase Concentration (mg mL^{-1})		
	0.2	**0.4**	**0.8**
Total number concentration (cm^{-3})	331,722±8,797	354,047±21,904	480,297±16,364
Average size (nm)	40.3±1.1	43.8±1.2	47.8±0.5
Mode (nm)	31.1	33.4	42.9
Median (nm)	33.4	35.9	39.0

4.4.2 Fullerene Collection Efficiency

We considered two flow rates in testing the impinger's nanoparticle collection efficiency. The efficiency achieved with the larger flow rate of 3.0 L min^{-1} was very low or even negative in most cases (results not shown). The results now focus on the flow rate of 0.1 L min^{-1}. Figure 4.9 shows collection efficiency for three consecutive sampling periods in green, blue, and black on the left axis as a function of particle size. Each panel represents a different initial aqueous concentration and/or stirring duration, and each presents the average collection efficiency for three time intervals after flow was initially diverted through the impinger. The initial particle

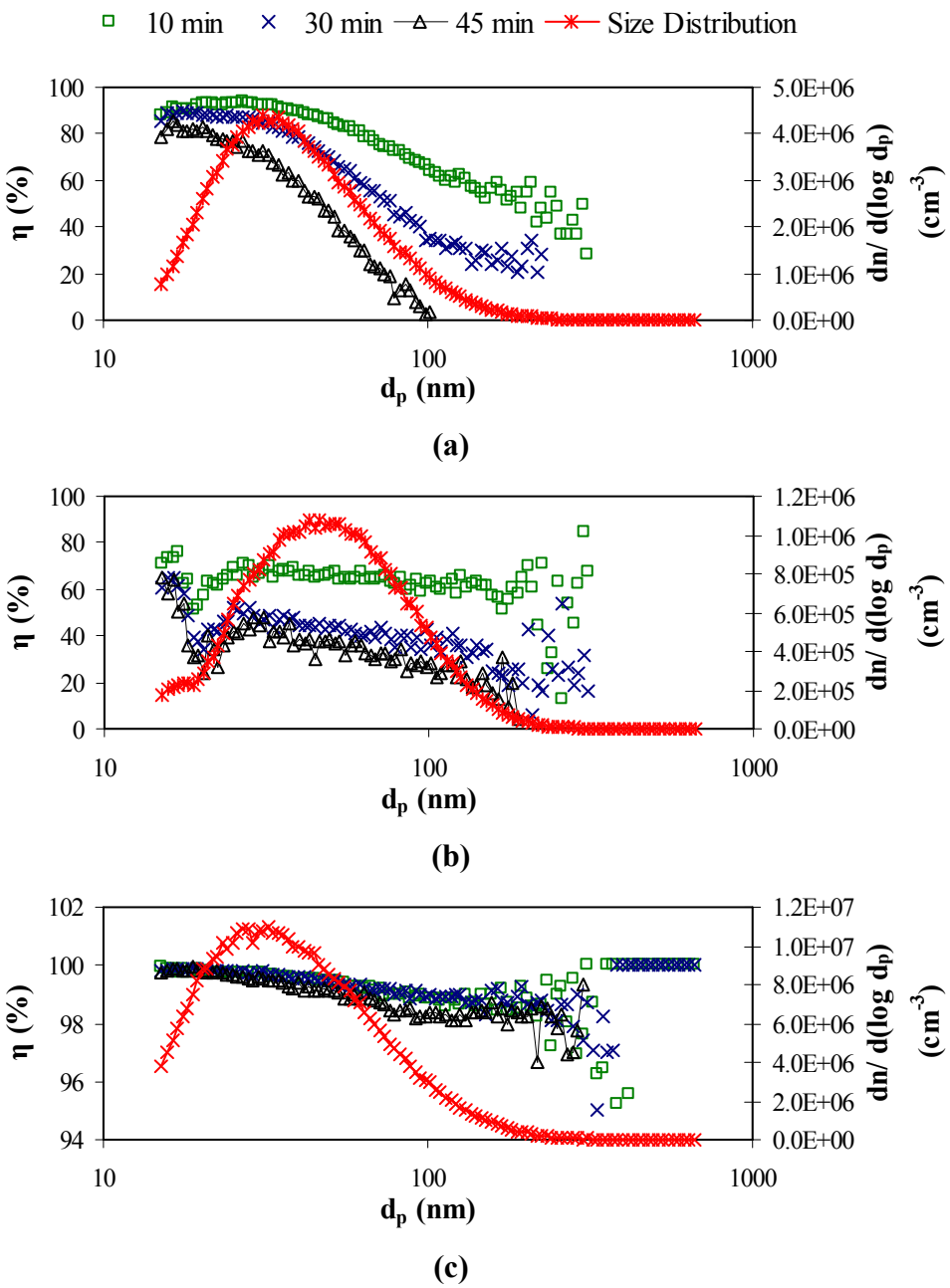

Figure 4.9. Collection efficiency (η) of aerosolized nC_{60} fullerene particles as a function of particle size, and initial size distribution for different aqueous-phase concentrations and stirring durations: a) 0.4 mg mL^{-1} after 2 weeks, b) 0.8 mg mL^{-1} after 2 weeks, c) 0.8 mg mL^{-1} after 4 months.

three time intervals after flow was initially diverted through the impinger. The initial particle size distribution, determined with aerosol flowing through the bypass route, is shown in red along the right axis. The collection efficiency is higher for smaller particles and highest for the

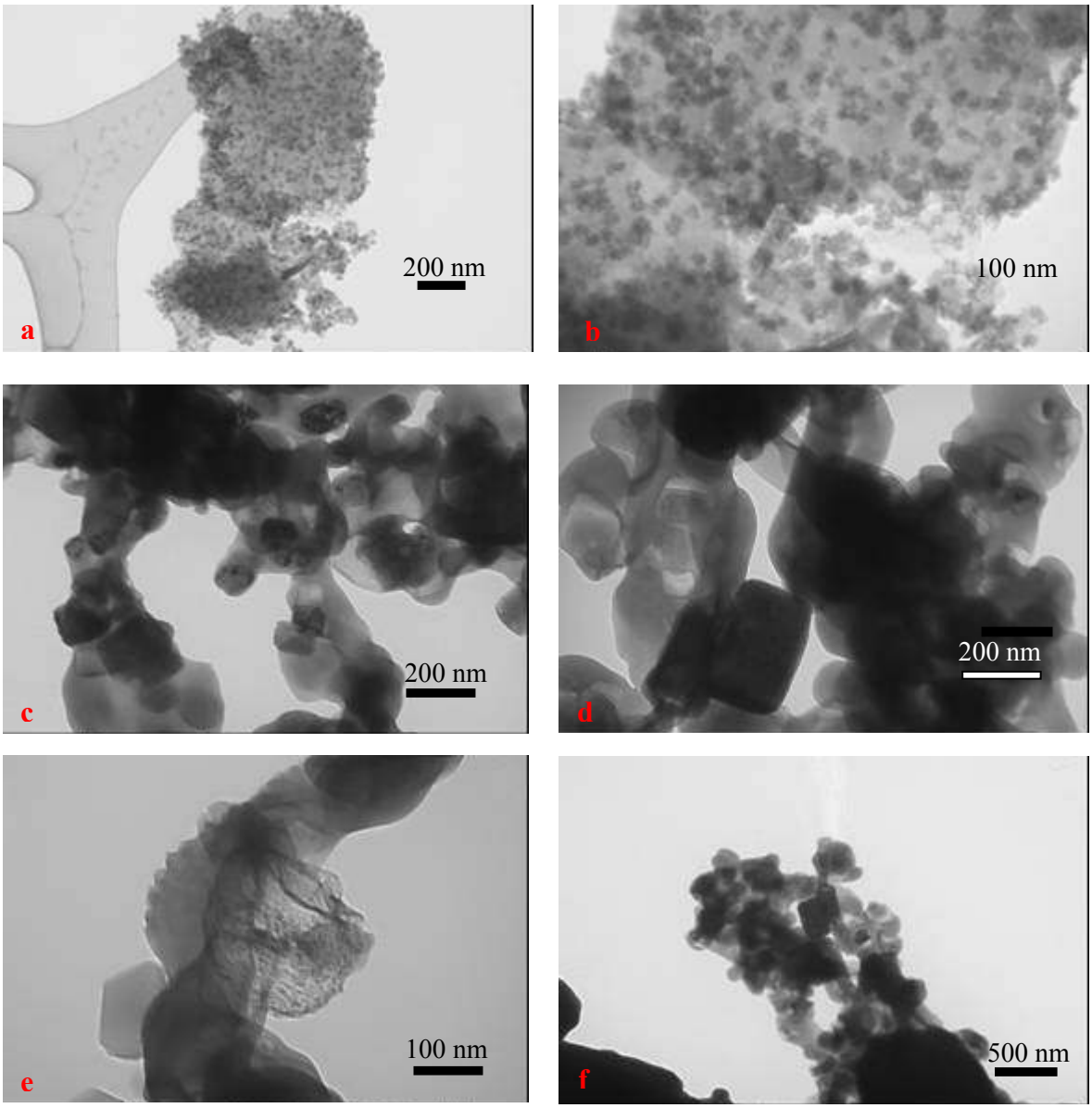

Figure 4.10. Representative TEM images of aerosolized nC_{60} aggregates for different aqueous-phase concentrations and stirring durations: a, b) 0.4 mg mL^{-1} after 2 weeks on Lacey TEM grids, c-e) 0.4 mg mL^{-1} after 2 weeks on Carbon/Formvar TEM grids, f) 0.8 mg mL^{-1} after 4 months on Carbon/Formvar TEM grids.

sample with an initial concentration of 0.8 mg mL^{-1} and stirring period of 4 months, with a value of 99.5% for particles with the mode diameter of 32.2 nm. It is of medium value for the sample with an initial concentration of 0.4 mg mL^{-1}: 72.4% for particles with the mode diameter of 31.1 nm. Finally, the collection efficiency is lowest for the sample with an initial concentration of 0.8

mg mL^{-1} and stirring period of 2 weeks: 37.6% for particles with the mode diameter of 46.1 nm. The figure also indicates that collection efficiency decreases over time.

Figure 4.10 shows TEM images of aerosolized nC_{60}. The particles' shapes and sizes vary; some, but not all have a well-defined facet. All of the aggregates shown in these images are substantially larger than the median particle size detected by the SMPS.

4.5 DISCUSSION

Figure 4.7 and Figure 4.8.b show that aerosolized particles have a relatively stable size distribution with the mean diameter increasing from 40.3 nm to 47.8 nm as the initial aqueous-phase concentration increases by a factor of four. A small increase in mean diameter with the initial aqueous-phase concentration is expected due to a higher rate of coagulation in the aerosolization system tubing with higher number concentrations of particles. As suggested by Deguchi et al. (2001), at higher aqueous-phase concentrations, nC_{60} clusters do not grow in size with the addition of more C_{60}, but instead form new clusters of the same size. Figure 4.8.a shows that the number concentration of particles increases with the aqueous-phase concentration, further supporting our assumption that clusters of the same size are being generated rather than larger size particles, if the aerosolized particles do in fact represent the most basic unit of nC_{60}. It is possible that an equilibrium aggregate size exists that balances growth by further attachment against shrinkage by loss of individual molecules.

The diameters of aerosolized nanoparticles are significantly smaller than reported for these particles in water, where the mean diameter of nC_{60} prepared by extended stirring in water is >170 nm (Brant et al. 2005a; Brant et al. 2005b; Dhawan et al. 2006). We hypothesize that the

shear forces experienced by nC_{60} as it is aerosolized may be sufficient to break apart the clusters of aggregates but are insufficient to shear off individual C_{60} molecules from a single aggregate. Such a mechanism would suggest that the larger size of particles in water is due to clustering of smaller nC_{60} aggregates, rather than growth in the size of crystals. Aggregated clusters are more easily broken apart by mechanical forces.

Figure 4.10 shows that aerosolized nC_{60} particles collected on the TEM grids are larger than the majority of those aerosolized (Figure 4.7 and Figure 4.9). Our method of collecting particles, passive placement of TEM grids in the sample tubing, may have favored impaction and interception as collection mechanisms. These two mechanisms act on larger particles and are ineffective for smaller particles ($d_p < 100$ nm). The shapes of the particles collected vary widely; some have a well-defined facet while others do not. Previous descriptions of nC_{60} in water report them to be spherical (Andrievsky et al. 2002; Andrievsky et al. 1999) and hexagonal or pentagonal with well-defined facets (Brant et al. 2005c). The observations from our experimental study suggest that aggregate formation resembles a process of crystal growth as well as undirected particle aggregation. A more effective method for collecting nanoparticles on TEM grids involves a thermophoretic precipitator (Gonzalez et al. 2005; Messerer et al. 2004; Murr and Soto 2005), which we are currently developing. Further study is needed to ensure that airborne nanoparticles are collected in a representative manner, for assessing their morphology by electron microscopy. Additionally, the type of TEM grid is also believed to impact the shape of collected particles. Figure 4.10 shows that the particles collected on Carbon/Formvar grids appear to be more fused than those collected on Lacey grids.

The main collection mechanism for particles in liquid impingers is traditionally considered to be impaction (Grinshpun et al. 1997). If a particle has sufficient inertia as it exits the impactor's nozzle in a bubble, it will either impact directly into the liquid or against the bottom surface of the reservoir. Collection efficiencies in impactors have been treated as monotonically increasing functions of particle inertia, i.e. mass and velocity. Therefore, an increase in flow rate through the impinger should result in a collection efficiency that asymptotically approaches 100% for a given particle size (Grinshpun et al. 1997; Lin et al. 1997).

However, this logic is only valid for larger particles. The dominant collection mechanism for nanoscale particles is diffusion via Brownian motion (Hogan et al. 2005), which increases with decreasing particle size. For smaller particles, a decreased flow rate will promote the formation of smaller bubbles, which will have longer residence times inside the liquid reservoir. Particles will then have more time to diffuse a farther distance (Einsteinn-Smoluchowski relationship for Brownian motion) from the bulk volume of the bubble to the air-water interface. Furthermore, the distance they need to diffuse to reach the air-water interface would be less in a smaller bubble.

The impinger's collection efficiency with a higher flow rate, 3.0 versus 0.1 L min^{-1}, was near-zero or even negative in some cases for nanoparticles. The negative values indicate that water in the reservoir itself aerosolizes and contributes to airborne particle concentrations. A lower flow rate of 0.1 L min^{-1} in the impinger results in a significant improvement in the collection efficiency of airborne nC_{60} by water. A larger volume of collection fluid, and therefore longer

residence time of bubbles, also contributes to increased collection efficiency as compared to other studies (Grinshpun et al. 1997; Lin et al. 1997).

As shown in Figure 4.9a and Figure 4.9b, the collection efficiency of sub-100 nm particles is lower for samples with higher initial aqueous-phase fullerene concentrations. The reason for this relationship is not known.

Comparison of the collection rates presented in Figure 4.9b and Figure 4.9c suggests that collection efficiency increases for an extended stirring period of 4 months versus 2 weeks. Brant et al. (2005a) report that nC_{60} prepared by stirring are hydrophilic. There has been no study on the effect of mixing period on the changes in the hydrophobicity of nC_{60} aggregates. However, Dhawan et al. (2006) show that the size of nC_{60} colloids and their zeta potential increases with mixing time. We hypothesize that extending the stirring period may increase the hydrophilicity of the particles and make them more easily transferred to water. Figure 4.6. shows that nC_{60} particles become more uniform in shape as the stirring period lengthens. The change might be due to changes in physicochemical characteristics of fullerene clusters. If this is the case, the results shown here are in agreement with those of Tseng and Li (2005) and Grinshpun et al. (1997). They suggest that impinger collection efficiencies are lower and reaerosolization rates higher for more hydrophobic particles. However, further studies are required to investigate the changes in the physicochemical characteristics of fullerene clusters that may occur is a function of mixing time.

Similar to the results of other studies (Grinshpun et al. 1997; Hogan et al. 2005; Lin et al. 1997),

the results of the current study also show that the collection efficiency of particles decreases as a function of time, due to evaporation losses and aerosolization of the sampling liquid.

4.6 CONCLUSION

We have demonstrated a method for aerosolizing manufactured nanomaterials and producing particles that are nanoscale in size. In this study, we investigated the physical characteristics of aerosolized C_{60} fullerene samples and their collection efficiency using a water-filled impinger. Three different concentrations of nC_{60} samples were prepared for the characterization study. The results showed that aerosolized particles have a relatively stable size distribution with a mean diameter of 40-48 nm and a mode of 31-43 nm, which is significantly smaller than the size reported for these particles in water, >170 nm. As the initial aqueous-phase concentration of samples increases, the average size of aerosolized particles remains relatively constant while the total number concentration of particles increases. If aerosolized particles represent the most basic unit of nC_{60}, then two scenarios may explain this behavior. First, this result may suggest that nC_{60} clusters in water do not grow in size by further attachment of more C_{60} molecules, but instead, new clusters of the same size are formed. Second, it might be possible that there exists an equilibrium size that balances growth by further attachment against shrinkage by loss of individual molecules.

To study the collection efficiency of carbonaceous nanoparticles in water, we prepared samples at two different concentrations with two different stirring durations. In general, very high efficiency was achieved for particles smaller than 100 nm. Decreasing the flow rate significantly improved the collection efficiency of nanoparticles. Enhancement of the hydrophilicity of

carbonaceous particles after extended mixing in water is also expected to be a factor in improving the collection efficiency of these particles. Further studies, however, are required to fully investigate the physical and chemical characteristics of nC_{60} aggregates after extended mixing in water.

To the best of our knowledge, this is the first investigation that characterizes the physical properties of carbonaceous nanoparticles aerosolized from an aqueous solution and their collection efficiency by stripping in water.

4.7 ACKNOWLEDGMENTS

This work was supported by grants from the National Science Foundation and the Virginia Tech ASPIRES program and by a Sussman Foundation fellowship to B. Yeganeh Talab. We would like to thank Steve McCartney at Macromolecule & Interfaces Institute of Virginia Tech for his technical support on the TEM studies.

4.8 REFERENCES

Alargova, R. G., Deguchi, S., and Tsujii, K. (2001). "Stable colloidal dispersions of fullerenes in polar organic solvents." *Journal of the American Chemical Society*, 123(43), 10460-10467.

Andrievsky, G. V., Klochkov, V. K., Bordyuh, A. B., and Dovbeshko, G. I. (2002). "Comparative analysis of two aqueous-colloidal solutions of C-60 fullerene with help of FTIR reflectance and UV-Vis spectroscopy." *Chemical Physics Letters*, 364(1-2), 8-17.

Andrievsky, G. V., Klochkov, V. K., Karyakina, E. L., and McHedlov-Petrossyan, N. O. (1999). "Studies of aqueous colloidal solutions of fullerene C-60 by electron microscopy." *Chemical Physics Letters*, 300(3-4), 392-396.

Andrievsky, G. V., Kosevich, M. V., Vovk, O. M., Shelkovsky, V. S., and Vashchenko, L. A. (1995). "On the Production of an Aqueous Colloidal Solution of Fullerenes." *Journal of the Chemical Society-Chemical Communications*(12), 1281-1282.

Brant, J., Labille, J., Bottero, J., and Wiesner, M. (2005a). "Differential Characteristics of fullerene nanoclusters produced through differential techniques." *Environmental Nanotechnology*, 729-735.

Brant, J., Lecoanet, H., Hotze, M., and Wiesner, M. (2005b). "Comparison of electrokinetic properties of colloidal fullerenes (n-C-60) formed using two procedures." *Environmental Science & Technology*, 39(17), 6343-6351.

Brant, J., Lecoanet, H., and Wiesner, M. R. (2005c). "Aggregation and deposition characteristics of fullerene nanoparticles in aqueous systems." *Journal of Nanoparticle Research*, 7(4-5), 545-553.

Brant, J. A., Labille, J., Bottero, J. Y., and Wiesner, M. R. (2006). "Characterizing the impact of preparation method on fullerene cluster structure and chemistry." *Langmuir*, 22(8), 3878-3885.

Deguchi, S., Alargova, R. G., and Tsujii, K. (2001). "Stable dispersions of fullerenes, C-60 and C-70, in water. Preparation and characterization." *Langmuir*, 17(19), 6013-6017.

Dhawan, A., Taurozzi, J. S., Pandey, A. K., Shan, W. Q., Miller, S. M., Hashsham, S. A., and Tarabara, V. V. (2006). "Stable colloidal dispersions of C-60 fullerenes in water: Evidence for genotoxicity." *Environmental Science & Technology*, 40(23), 7394-7401.

Donaldson, K., Li, X. Y., and MacNee, W. (1998). "Ultrafine (nanometre) particle mediated lung injury." *Journal of Aerosol Science*, 29(5-6), 553-560.

Fortner, J. D., Lyon, D. Y., Sayes, C. M., Boyd, A. M., Falkner, J. C., Hotze, E. M., Alemany, L. B., Tao, Y. J., Guo, W., Ausman, K. D., Colvin, V. L., and Hughes, J. B. (2005). "C-60 in water: Nanocrystal formation and microbial response." *Environmental Science & Technology*, 39(11), 4307-4316.

Gonzalez, D., Nasibulin, A. G., Baklanov, A. M., Shandakov, S. D., Brown, D. P., Queipo, P., and Kauppinen, E. I. (2005). "A new thermophoretic precipitator for collection of nanometer-sized aerosol particles." *Aerosol Science and Technology*, 39(11), 1064-1071.

Grinshpun, S. A., Willeke, K., Ulevicius, V., Juozaitis, A., Terzieva, S., Donnelly, J., Stelma, G. N., and Brenner, K. P. (1997). "Effect of impaction, bounce and reaerosolization on the collection efficiency of impingers." *Aerosol Science and Technology*, 26(4), 326-342.

Gwinn, M. R., and Vallyathan, V. (2006). "Nanoparticles: Health effects - Pros and cons." *Environmental Health Perspectives*, 114(12), 1818-1825.

Hogan, C. J., Kettleson, E. M., Lee, M. H., Ramaswami, B., Angenent, L. T., and Biswas, P. (2005). "Sampling methodologies and dosage assessment techniques for submicrometre and ultrafine virus aerosol particles." *Journal of Applied Microbiology*, 99(6), 1422-1434.

Jia, G., Wang, H. F., Yan, L., Wang, X., Pei, R. J., Yan, T., Zhao, Y. L., and Guo, X. B. (2005). "Cytotoxicity of carbon nanomaterials: Single-wall nanotube, multi-wall nanotube, and fullerene." *Environmental Science & Technology*, 39(5), 1378-1383.

Kim, D. S., Lim, K. S., Xiang, R. B., and Lee, K. W. (2002). "Design and performance evaluation of an aerosol separator." *Journal of Aerosol Science*, 33(10), 1405-1415.

Kim, S., Jaques, P. A., Chang, M. C., Barone, T., Xiong, C., Friedlander, S. K., and Sioutas, C. (2001). "Versatile aerosol concentration enrichment system (VACES) for simultaneous in vivo and in vitro evaluation of toxic effects of ultrafine, fine and coarse ambient particles - Part II: Field evaluation." *Journal of Aerosol Science*, 32(11), 1299-1314.

Lam, C. W., James, J. T., McCluske, R., and Hunter, R. L. (2004). "Pulmonary toxicity of single-wall carbon nanotubes in mice 7 and 90 days after intratracheal instillation." *Toxicological Sciences*, 77, 9.

Lin, X. J., Willeke, K., Ulevicius, V., and Grinshpun, S. A. (1997). "Effect of sampling time on the collection efficiency of all-glass impingers." *American Industrial Hygiene Association Journal*, 58(7), 480-488.

Maynard, A. D., and Kuempel, E. D. (2005). "Airborne nanostructured particles and occupational health." *Journal of Nanoparticle Research*, 7(6), 587-614.

McHedlov-Petrossyan, N. O., Klochkov, V. K., and Andrievsky, G. V. (1997). "Colloidal dispersions of fullerene C-60 in water: some properties and regularities of coagulation by electrolytes." *Journal of the Chemical Society-Faraday Transactions*, 93(24), 4343-4346.

Messerer, A., Niessner, R., and Poschl, U. (2004). "Miniature pipe bundle heat exchanger for thermophoretic deposition of ultrafine soot aerosol particles at high flow velocities." *Aerosol Science and Technology*, 38(5), 456-466.

Murr, L. E., and Soto, K. F. (2005). "A TEM study of soot, carbon nanotubes, and related fullerene nanopolyhedra in common fuel-gas combustion sources." *Materials Characterization*, 55(1), 50-65.

Oberdörster, E. (2004). "Manufactured nanomaterials (Fullerenes, C-60) induce oxidative stress in the brain of juvenile largemouth bass." *Environmental Health Perspectives*, 112(10), 1058-1062.

Oberdörster, G. (2000). "Toxicology of ultrafine particles: in vivo studies." *Philosophical Transactions of the Royal Society of London Series a-Mathematical Physical and Engineering Sciences*, 358(1775), 2719-2739.

Oberdörster, G. (2001). "Pulmonary effects of inhaled ultrafine particles." *International Archives of Occupational and Environmental Health*, 74(1), 1-8.

Oberdorster, G., Gelein, R. M., Ferin, J., and Weiss, B. (1995). "Association of Particulate Air-Pollution and Acute Mortality - Involvement of Ultrafine Particles." *Inhalation Toxicology*, 7(1), 111-124.

Oberdörster, G., Oberdörster, E., and Oberdörster, J. (2005). "Nanotoxicology: An emerging discipline evolving from studies of ultrafine particles." *Environmental Health Perspectives*, 113(7), 823-839.

Peters, A., Wichmann, E., Tuch, T., Heinrich, J., and Heyder, J. (1997). "Respiratory effects are associated with the number of ultrafine particles." *American Journal of Respiratory and Critical Care Medicine*, 155, 18.

Pope, C. A., Burnett, R. T., Thun, M. J., Calle, E. E., Krewski, D., Ito, K., and Thurston, G. D. (2002). "Lung cancer, cardiopulmonary mortality, and long-term, exposure to fine particulate air pollution." *Journal of the American Medical Association*, 287, 10.

Roco, M. C. (2005). "Environmentally responsible development of nanotechnology." *Environmental Science & Technology*, 39(5), 106A-112A.

Seinfeld, J. H., and Pandis, S. N. (2006). *Atmospheric chemistry and physics*.

Spanne, M., Grzybowski, P., and Bohgard, M. (1999). "Collection efficiency for submicron particles of a commonly used impinger." *American Industrial Hygiene Association Journal*, 60(4), 540-544.

Tseng, C. C., and Li, C. S. (2005). "Collection efficiencies of aerosol samplers for virus-containing aerosols." *Journal of Aerosol Science*, 36(5-6), 593-607.

Tsuji, J. S., Maynard, A. D., Howard, P. C., James, J. T., Lam, C. W., Warheit, D. B., and Santamaria, A. B. (2006). "Research strategies for safety evaluation of nanomaterials, part IV: Risk assessment of nanoparticles." *Toxicological Sciences*, 89(1), 42-50.

Warheit, D. B., Laurence, B. R., Reed, K. L., Roach, D. H., Reynolds, G. A. M., and Webb, T. R. (2004). "Comparative pulmonary toxicity assessment of single-wall carbon nanotubes in rats." *Toxicological Sciences*, 77(9), 117.

Weibel, A., Bouchet, R., Boulc'h, F., and Knauth, P. (2005). "The big problem of small particles: A comparison of methods for determination of particle size in nanocrystalline anatase powders." *Chemistry of Materials*, 17(9), 2378-2385.

Wiesner, M. R., Lowry, G. V., Alvarez, P., Dionysiou, D., and Biswas, P. (2006). "Assessing the risks of manufactured nanomaterials." *Environmental Science & Technology*, 40(14), 4336-4345.

Willeke, K., Lin, X. J., and Grinshpun, S. A. (1998). "Improved aerosol collection by combined impaction and centrifugal motion." *Aerosol Science and Technology*, 28(5), 439-456.

CHAPTER 5

CONCLUSIONS AND RECOMMENDATIONS

5.1 SUMMARY

Despite the rapid growth in nanotechnology, very little is known about the unintended health or environmental effects of manufactured nanomaterials. As a first step in assessing the risk associated with nanoparticles, we conducted a set of field studies to investigate the concentrations and size distributions of airborne particles in two nanomaterial manufacturing facilities. Furthermore, we demonstrated a method for generating airborne nanoparticles from the aqueous-phase suspensions and then investigated the collection efficiency of nanosize carbonaceous airborne particles in water using an impinger.

5.2 CONCLUSIONS

The conclusions of the research study presented in this manuscript can be summarized as follows:

5.2.1 Exposure to Airborne Nanoparticles During Production of Carbonaceous Nanomaterials in the Workplace

We have investigated the potential risk of exposure to airborne particles in two nanomaterials manufacturing facilities, a commercial plant and a university laboratory. Measurements were performed at three different locations, i.e. *near reactor*, *breathing zone*, and *background*, at

different steps of the manufacturing process. We found that physical handling of the material, either by sweeping or vacuuming, results in elevated concentrations of $PM_{2.5}$ and particle number. In both facilities, the increase in total number concentration of particles ($d_p < 673$ nm) can be attributed mainly to an increase in the number of particles smaller than 100 nm, so nanoparticles are clearly suspended during such activities. Physical activities of the workers also results in the suspension of larger particles. As expected, containment of the reactor inside a fume hood partially limits the spreading of nanoparticles throughout the facility. This study contributes important new data regarding exposure to engineered nanoparticles.

5.2.2 Aerosolization of C_{60} Fullerene and Its Collection in Water Using an Impinger

We have demonstrated a method for aerosolizing manufactured nanomaterials and producing particles that are nanoscale in size. In this study, we investigated the physical characteristics of aerosolized C_{60} fullerenes and their collection efficiency in a water-filled impinger. Three different concentrations of nC_{60} samples were prepared for the characterization study. The results showed that aerosolized particles have a relatively stable size distribution with a mean diameter of 40-48 nm and a mode of 31-43 nm, which is significantly smaller than the size reported for these particles in water, >170 nm. The aerosolization process appears to break up the nC_{60} clusters into fairly uniform sizes. As the initial aqueous-phase concentration of samples increases, the average size of aerosolized particles stays relatively constant while the total number concentration of particles increases.

To study the collection efficiency of carbonaceous nanoparticles in water, we prepared samples at two different concentrations with two different stirring durations, aerosolized the samples, and

then bubbled the aerosol through an impinger in attempt to return the particles to the aqueous phase. In general, very high collection efficiency in the impinger was achieved for particles smaller than 100 nm, when we used a flow rate of 0.1 L min^{-1}. The results further confirm that Brownian diffusion is the main mechanism of collection for very small particles in an impinger. Decreasing the flow rate significantly improved the collection efficiency of nanoparticles. Enhancement of the hydrophilicity of carbonaceous particles after extended mixing in water is also expected to be a factor in improving the collection efficiency of these particles. Further studies, however, are required to fully investigate the physical and chemical characteristics of C_{60} particles after extended mixing in water.

To the best of our knowledge, this is the first investigation that characterizes the physical properties of carbonaceous nanoparticles aerosolized from an aqueous solution and their collection efficiency by stripping in water.

5.3 LIMITATIONS OF PRESENT STUDY

The results presented in this manuscript for the exposure to airborne nanoparticles in a nanotechnology workplace are only valid for the investigated sites and for carbonaceous nanomaterials. Results from other sites and other types of nanomaterials are needed to support the development of guidelines and regulations to protect human health and the environment.

Additionally, the sampling techniques used in this study do not differentiate between particles generated by nanomaterials soot production and those from other sources. Differences across production runs (time of day) and space may reflect the presence of other particle sources in the

room, such as drilling and personal dust resuspension, changes in ventilation of the room, and/or changes in ambient concentrations throughout the day. Due to equipment limitations, we sampled at each location in series and were not able to obtain simultaneous measurements in multiple locations except for continuous *background* measurements in the commercial plant on one day.

Measured exposures showed variation in total number concentration of particles in different locations of the university laboratory that can not be explained by physical handling or dispersion of the manufactured nanomaterials. Further investigations are required to clarify the reasons for lower total number concentrations of fine particles in the *breathing zone* as compared to the *near reactor* and *background* locations during the sweeping period.

Initial results for the collection efficiency of carbonaceous nanoparticles in water revealed very high efficiency for particles smaller than 100 nm at a low air flow rate. Enhancement of the hydrophilicity of carbonaceous particles after extended mixing in water is also expected to be a factor in improving the collection efficiency of these particles. Further studies, however, are required to fully investigate the physical and chemical characteristics of C_{60} particles after extended mixing in water.

The observations of airborne nanoparticles from our experimental study suggest that aggregate formation resembles a process of crystal growth as well as undirected particle aggregation. Further study is needed to ensure that airborne nanoparticles are collected in a representative manner, for assessing their morphologies by electron microscopy.

The information provided for characterizing properties of nanoparticles in airborne form is valid for the nC_{60} fullerene samples prepared by the method and concentrations presented in this investigation, and can not be generalized without further investigations.

5.4 RECOMMENDATIONS FOR FUTURE STUDIES

To address the limitations presented in the previous section, the following recommendations should be considered for continuing this line of research:

- Performing a computational fluid dynamics (CFD) model to study the air flow patterns inside a nanotechnology workplace.

- Collecting simultaneous measurements of airborne nanoparticles in multiple locations within a nanotechnology workplace.

- Developing a method to distinguish between the nanomaterial of interest versus other airborne particles, and executing further investigation including chemical analysis to facilitate source apportionment of airborne particles in the nanotechnology workplace.

- Studying the changes in the physicochemical characteristics of fullerene clusters as a function of mixing time.

- Conducting impinger experiments at additional low air flow rates, and defining the relationship between flow rate and collection efficiency for nanoparticles.

- Developing a more effective method for collecting nanoparticles on TEM grids.

LIST OF REFERENCES

Adgate, J. L., Ramachandran, G., Pratt, G. C., Walker, L. A., and Sexton, K. (2002). "Spatial and temporal variability in outdoor, indoor and personal $PM_{2.5}$ exposure." *Atmospheric Environment*, 36, 11.

Aitken, R. J., Chaudhry, M. Q., Boxall, A. B. A., and Hull, M. (2006). "Manufacture and use of nanomaterials: current status in the UK and global trends." *Occupational Medicine-Oxford*, 56(5), 300-306.

Alargova, R. G., Deguchi, S., and Tsujii, K. (2001). "Stable colloidal dispersions of fullerenes in polar organic solvents." *Journal of the American Chemical Society*, 123(43), 10460-10467.

Andrievsky, G. V., Klochkov, V. K., Bordyuh, A. B., and Dovbeshko, G. I. (2002). "Comparative analysis of two aqueous-colloidal solutions of C-60 fullerene with help of FTIR reflectance and UV-Vis spectroscopy." *Chemical Physics Letters*, 364(1-2), 8-17.

Andrievsky, G. V., Klochkov, V. K., Karyakina, E. L., and McHedlov-Petrossyan, N. O. (1999). "Studies of aqueous colloidal solutions of fullerene C-60 by electron microscopy." *Chemical Physics Letters*, 300(3-4), 392-396.

Andrievsky, G. V., Kosevich, M. V., Vovk, O. M., Shelkovsky, V. S., and Vashchenko, L. A. (1995). "On the Production of an Aqueous Colloidal Solution of Fullerenes." *Journal of the Chemical Society-Chemical Communications*(12), 1281-1282.

Bennett, D. H., and Koutrakis, P. (2006). "Determining the infiltration of outdoor particles in the indoor environment using a dynamic model." *Journal of Aerosol Science*, 37(6), 20.

Borm, P. J. A. (2002). "Particle toxicology: from coal mining to nanotechnology." *Inhalation Toxicology*, 14, 14.

Borm, P. J. A., and Kreyling, W. (2004). "Toxicological hazards of inhaled nanoparticles-potential implications for drug delivery." *Journal of Nanoscience and Nanotechnology*, 4, 11.

Brant, J., Labille, J., Bottero, J., and Wiesner, M. (2005a). "Differential Characteristics of fullerene nanoclusters produced through differential techniques." *Environmental Nanotechnology*, 729-735.

Brant, J., Lecoanet, H., Hotze, M., and Wiesner, M. (2005b). "Comparison of electrokinetic properties of colloidal fullerenes (n-C-60) formed using two procedures." *Environmental Science & Technology*, 39(17), 6343-6351.

Brant, J., Lecoanet, H., and Wiesner, M. R. (2005c). "Aggregation and deposition characteristics of fullerene nanoparticles in aqueous systems." *Journal of Nanoparticle Research*, 7(4-5), 545-553.

Brant, J. A., Labille, J., Bottero, J. Y., and Wiesner, M. R. (2006). "Characterizing the impact of preparation method on fullerene cluster structure and chemistry." *Langmuir*, 22(8), 3878-3885.

Brouwer, D. H., Gijsbers, J. H. J., and Lurvink, M. W. M. (2004). "Personal exposure to ultrafine particles in the workplace: Exploring sampling techniques and strategies." *Annals of Occupational Hygiene*, 48(5), 439-453.

Colvin, V. L. (2003). "The potential environmental impact of engineered nanomaterials." *nature Biotechnology*, 21, 5.

Deguchi, S., Alargova, R. G., and Tsujii, K. (2001). "Stable dispersions of fullerenes, C-60 and C-70, in water. Preparation and characterization." *Langmuir*, 17(19), 6013-6017.

Dhawan, A., Taurozzi, J. S., Pandey, A. K., Shan, W. Q., Miller, S. M., Hashsham, S. A., and Tarabara, V. V. (2006). "Stable colloidal dispersions of C-60 fullerenes in water: Evidence for genotoxicity." *Environmental Science & Technology*, 40(23), 7394-7401.

Donaldson, K., Li, X. Y., and MacNee, W. (1998). "Ultrafine (nanometre) particle mediated lung injury." *Journal of Aerosol Science*, 29(5-6), 553-560.

Donaldson, K., Stone, V., Gilmour, P. S., Brown, D. M., and MacNee, W. (2000). "Ultrafine particles: mechanisms of lung injury." *Philosophical Transactions of the Royal Society of London Series a-Mathematical Physical and Engineering Sciences*, 358(1775), 2741-2748.

Ferro, A., Kopperud, R. J., and Hildemann, L. M. (2004). "Elevated personal exposure to particulate matter from human activities in a residence." *Journal of Exposure Analysis and Environmental Epidemiology*, 14, 7.

Fortner, J. D., Lyon, D. Y., Sayes, C. M., Boyd, A. M., Falkner, J. C., Hotze, E. M., Alemany, L. B., Tao, Y. J., Guo, W., Ausman, K. D., Colvin, V. L., and Hughes, J. B. (2005). "C-60 in water: Nanocrystal formation and microbial response." *Environmental Science & Technology*, 39(11), 4307-4316.

Gonzalez, D., Nasibulin, A. G., Baklanov, A. M., Shandakov, S. D., Brown, D. P., Queipo, P., and Kauppinen, E. I. (2005). "A new thermophoretic precipitator for collection of nanometer-sized aerosol particles." *Aerosol Science and Technology*, 39(11), 1064-1071.

Grinshpun, S. A., Willeke, K., Ulevicius, V., Juozaitis, A., Terzieva, S., Donnelly, J., Stelma, G. N., and Brenner, K. P. (1997). "Effect of impaction, bounce and reaerosolization on the collection efficiency of impingers." *Aerosol Science and Technology*, 26(4), 326-342.

Gwinn, M. R., and Vallyathan, V. (2006). "Nanoparticles: Health effects - Pros and cons." *Environmental Health Perspectives*, 114(12), 1818-1825.

Hogan, C. J., Kettleson, E. M., Lee, M. H., Ramaswami, B., Angenent, L. T., and Biswas, P. (2005). "Sampling methodologies and dosage assessment techniques for submicrometre and ultrafine virus aerosol particles." *Journal of Applied Microbiology*, 99(6), 1422-1434.

Hovorka, J., Holub, R. F., Branis, M., and Honeyman, B. D. (2005). "Tracing outdoor/indoor penetration of PM2.5, PM1.0 by Po-210/Pb-210." *Indoor and Built Environment*, 14(3-4), 5.

Jia, G., Wang, H. F., Yan, L., Wang, X., Pei, R. J., Yan, T., Zhao, Y. L., and Guo, X. B. (2005). "Cytotoxicity of carbon nanomaterials: Single-wall nanotube, multi-wall nanotube, and fullerene." *Environmental Science & Technology*, 39(5), 1378-1383.

Kim, D. S., Lim, K. S., Xiang, R. B., and Lee, K. W. (2002). "Design and performance evaluation of an aerosol separator." *Journal of Aerosol Science*, 33(10), 1405-1415.

Lam, C. W., James, J. T., McCluske, R., and Hunter, R. L. (2004). "Pulmonary toxicity of single-wall carbon nanotubes in mice 7 and 90 days after intratracheal instillation." *Toxicological Sciences*, 77, 9.

Lin, X. J., Willeke, K., Ulevicius, V., and Grinshpun, S. A. (1997). "Effect of sampling time on the collection efficiency of all-glass impingers." *American Industrial Hygiene Association Journal*, 58(7), 480-488.

Liu, L. J. S., Box, M., Kalman, D., Kaufman, J., Koenig, J., Larson, T., Lumley, T., Sheppard, L., and Wallace, L. (2003). "Exposure assessment of particulate matter for susceptible population in Seattle." *Environmental Health Perspectives*, 111, 10.

Maynard, A. D., Baron, P. A., Foley, M., Shvedova, A. A., Kisin, E. R., and Castranova, V. (2004). "Exposure to carbon nanotube material: Aerosol release during the handling of unrefined single-walled carbon nanotube material." *Journal of Toxicology and Environmental Health-Part A*, 67(1), 87-107.

Maynard, A. D., and Kuempel, E. D. (2005). "Airborne nanostructured particles and occupational health." *Journal of Nanoparticle Research*, 7(6), 587-614.

McHedlov-Petrossyan, N. O., Klochkov, V. K., and Andrievsky, G. V. (1997). "Colloidal dispersions of fullerene C-60 in water: some properties and regularities of coagulation by electrolytes." *Journal of the Chemical Society-Faraday Transactions*, 93(24), 4343-4346.

Messerer, A., Niessner, R., and Poschl, U. (2004). "Miniature pipe bundle heat exchanger for thermophoretic deposition of ultrafine soot aerosol particles at high flow velocities." *Aerosol Science and Technology*, 38(5), 456-466.

Murr, L. E., and Soto, K. F. (2005). "A TEM study of soot, carbon nanotubes, and related fullerene nanopolyhedra in common fuel-gas combustion sources." *Materials Characterization*, 55(1), 50-65.

Oberdörster, E. (2004). "Manufactured nanomaterials (Fullerenes, C-60) induce oxidative stress in the brain of juvenile largemouth bass." *Environmental Health Perspectives*, 112(10), 1058-1062.

Oberdörster, G. (2001). "Pulmonary effects of inhaled ultrafine particles." *International Archives of Occupational and Environmental Health*, 74(1), 1-8.

Oberdörster, G., Oberdörster, E., and Oberdörster, J. (2005). "Nanotoxicology: An emerging discipline evolving from studies of ultrafine particles." *Environmental Health Perspectives*, 113(7), 823-839.

Peters, A., Wichmann, E., Tuch, T., Heinrich, J., and Heyder, J. (1997). "Respiratory effects are associated with the number of ultrafine particles." *American Journal of Respiratory and Critical Care Medicine*, 155, 18.

Pope, C. A., Burnett, R. T., Thun, M. J., Calle, E. E., Krewski, D., Ito, K., and Thurston, G. D. (2002). "Lung cancer, cardiopulmonary mortality, and long-term, exposure to fine particulate air pollution." *Journal of the American Medical Association*, 287, 10.

Roco, M. C. (2005). "Environmentally responsible development of nanotechnology." *Environmental Science & Technology*, 39(5), 106A-112A.

Seinfeld, J. H., and Pandis, S. N. (2006). *Atmospheric chemistry and physics*.

Spanne, M., Grzybowski, P., and Bohgard, M. (1999). "Collection efficiency for submicron particles of a commonly used impinger." *American Industrial Hygiene Association Journal*, 60(4), 540-544.

Stevenson, S., Rice, G., Glass, T., Harich, K., Cromer, F., Jordan, M. R., Craft, J., Hadju, E., Bible, R., Olmstead, M. M., Maitra, K., Fisher, A. J., Balch, A. L., and Dorn, H. C. (1999). "Small-bandgap endohedral metallofullerenes in high yield and purity." *Nature*, 401, 55-57.

Tseng, C. C., and Li, C. S. (2005). "Collection efficiencies of aerosol samplers for virus-containing aerosols." *Journal of Aerosol Science*, 36(5-6), 593-607.

Tsuji, J. S., Maynard, A. D., Howard, P. C., James, J. T., Lam, C. W., Warheit, D. B., and Santamaria, A. B. (2006). "Research strategies for safety evaluation of nanomaterials, part IV: Risk assessment of nanoparticles." *Toxicological Sciences*, 89(1), 42-50.

van Poppel, L. H., Friedrich, H., Spinsby, J., Chung, S. H., Seinfeld, J. H., and Buseck, P. R. (2005). "Electron tomography of nanoparticle clusters: Implications for atmospheric lifetimes and radiative forcing of soot." *Geophysical Research Letters*, 32 Art. No. L24811.

Warheit, D. B., Laurence, B. R., Reed, K. L., Roach, D. H., Reynolds, G. A. M., and Webb, T. R. (2004). "Comparative pulmonary toxicity assessment of single-wall carbon nanotubes in rats." *Toxicological Sciences*, 77(9), 117.

Weibel, A., Bouchet, R., Boulc'h, F., and Knauth, P. (2005). "The big problem of small particles: A comparison of methods for determination of particle size in nanocrystalline anatase powders." *Chemistry of Materials*, 17(9), 2378-2385.

Wiesner, M. R., Lowry, G. V., Alvarez, P., Dionysiou, D., and Biswas, P. (2006). "Assessing the risks of manufactured nanomaterials." *Environmental Science & Technology*, 40(14), 4336-4345.

Willeke, K., Lin, X. J., and Grinshpun, S. A. (1998). "Improved aerosol collection by combined impaction and centrifugal motion." *Aerosol Science and Technology*, 28(5), 439-456.

Zhu, Y. F., Hinds, W. C., Krudysz, M., Kuhn, T., Froines, J., and Sioutas, C. (2005). "Penetration of freeway ultrafine particles into indoor environments." *Journal of Aerosol Science*, 36(3), 20.

APPENDIX A

Table A.1. $PM_{2.5}$ and particle size distributions (average ± standard deviation) in the commercial manufacturing plant.

Date	Location[a]	Activity	N[b] (cm^{-3})	Mean diameter[c] (nm)	SMPS scans	$PM_{2.5}$
Commercial manufacturing facility						
4 Aug 05	NR	Arc	NA	NA	NA	146±14
	NR	Sweep	5,352±832[d]	87±11[d]	11	152±25
	NR	Vacuum	5,339±408[d]	84±7[d]	2	147±5
	BZ	Arc	NA	NA	NA	119±6
	BZ	Sweep	4,834±925[d]	80±9[d]	11	124±7
	BZ	Vacuum	4,494±216[d]	74±4[d]	3	124±4
	BG	Arc	NA	NA	NA	122±3
	BG	Sweep	3,667±1,311[d]	100±13	11	128±13
	BG	Vacuum	9,843±978[d]	45±3	2	126±4
9 Aug 05	NR	Arc	NA	NA	NA	NA
	NR	Sweep	1,1306±1,765	60±6	14	92±128
	NR	Vacuum	8,240±1,165	68±7	2	36±3
	BZ	Arc	NA	NA	NA	NA
	BZ	Sweep	5,415±313	81±3	11	37±3
	BZ	Vacuum	5,878±835	76±6	2	32±4
	BG	Arc	NA	NA	NA	NA
	BG	Sweep	12,502±394	134±6	8	85±5
	BG	Vacuum	14,224±193	143±5	5	110±11
21 Jun 06	NR	Arc	75,484±35,087	62.2	61	52±4
	NR	Sweep	124,171±147,125	35.4	2	56±5
	NR	Vacuum	NA	NA	NA	NA
	BZ	Arc	50,115±6,426	41.9	23	52±12
	BZ	Sweep	6,9713±7,861	69.8	5	47±2
	BZ	Vacuum	NA	NA	NA	NA
	BG	Arc	63,932±43,721	75.6	49	86±68
	BG	Sweep	78,337±50,088 42,395±3,585	48.9 94.7	9 2	50±4
	BG	Vacuum	33,935±1,370	118	6	49±2
25 Jul 06	NR	Arc	110,146±30,676	45.3	32	81±14
	NR	Sweep	74,010±70,865	65.5	4	79±25
	NR	Vacuum	95,964±NA	50.3	1	85±3
	BZ	Arc	57,787±2,323	91.4	10	86±50
	BZ	Sweep	76,486±3,199	78.1	4	72±11
	BZ	Vacuum	NA	NA	NA	NA
	BG	Arc	35,038±7,786	85.1	31	55±3
	BG	Sweep	34,769±6,983	91.4	14	61±4
	BG	Vacuum	31,764±2,914	94.7	4	60±3

[a] Near reactor (NR), breathing zone (BZ), or background (BG).

[b] Total number concentration (arithmetic mean ± standard deviation across SMPS scans) in the size range 14-663 nm, unless otherwise indicated.

[c] Arithmetic mean ± standard deviation across SMPS scans.

[d] The SMPS was outfitted with a nano-DMA, which measures particles in the size range of 4-160 nm.

Table A.2. $PM_{2.5}$ and particle size distributions (average ± standard deviation) in the university laboratory.

Date	Location[a]	Activity	N[b] (cm^{-3})	Mean diameter[c] (nm)	SMPS Scans	$PM_{2.5}$
University Laboratory						
4 Oct 05[d]	BZ	Sweep	7,845±2,458	77±18	7	41±2
	BZ	Vacuum	6,762±276	96±10	2	42±3
	BZ	Sweep	9,835±2,962	87±6	6	39±3
	BZ	Vacuum	12,847±1,159	77±4	2	42±3
5 Oct 05[d]	NR	Sweep	3,269±361	53±3	3	24±36
	NR	Vacuum	3,858	48	1	28±49
	NR	Sweep	6,953±8,450[e]	53±14	5	53±134
	NR	Vacuum	4,192	35	1	9±5
28 Aug 06[d]	NR	Arc	54,997±9,756	66.1	30	66 ±2
	NR	Sweep	34,358±1,459	69.7	6	72±9
	NR	Vacuum	NA	NA	NA	NA
	NR	Arc	57,187±9,014	67.3	29	90 ±5
	NR	Sweep	59,791±2,962	102	5	100±14
	NR	Vacuum	NA	NA	NA	NA
	NR	Arc	43,912±8,338	94.7	33	89±3
	NR	Sweep	42,487±944	106	3	98±49
	NR	Vacuum	NA	NA	NA	NA
	NR	Arc	44,533±11,810	85.1	31	85±6
	NR	Sweep	39,630±983	98.2	3	78±10
	NR	Vacuum	NA	NA	NA	NA
29 Aug 06[d]	BZ	Arc	54,997±9,756	61.5	30	69±3
	BZ	Sweep	41,134±2,897	80.6	4	66±2
	BZ	Vacuum	NA	NA	NA	NA
	BZ	Arc	NA	NA	NA	53±5
	BZ	Sweep	20,599±1,390	91.4	4	45±2
	BZ	Vacuum	NA	NA	NA	NA
	BZ	Arc	57,187±9,014	69.8	29	39±3
	BZ	Sweep	28,099±10,749	84.2	5	38±2
	BZ	Vacuum	NA	NA	NA	NA
	BZ	Arc	43,912±8,338	55.2	33	26±4
	BZ	Sweep	NA	NA	NA	22±2
	BZ	Vacuum	NA	NA	NA	NA
	BZ	Arc	26,567±18,729	38.5	29	21±1
	BZ	Sweep	17,460±3,703	66.9	5	23±3
	BZ	Vacuum	NA	NA	NA	NA
30 Aug 06[d]	NR	Vacuum	NA	NA	NA	84±28
	BG	Arc	52,363±9,478	51.4	31	34±1
	BG	Sweep	50,048±4,758	53.3	5	37±1
	BG	Vacuum	NA	NA	NA	NA
	BG	Arc	31,741±9,254	75.1	33	48±6
	BG	Sweep	23,923±833	89.8	2	52±1
	BG	Vacuum	NA	NA	NA	NA
	BG	Arc	32,360±6,130	71.0	28	54±2

BG	Sweep	30,416±1,052	82	4	57±1
BG	Vacuum	NA	NA	NA	NA
BG	Arc	37,235±7,777	80.6	30	63±3
BG	Sweep	36,828±2,193	88.3	4	71±1
BG	Vacuum	NA	NA	NA	NA
BG	Arc	41,654±8,069	82.5	28	76±1
BG	Sweep	44,437±2,053	86.7	2	79±1
BG	Vacuum	NA	NA	NA	NA

[a] Near reactor (NR), breathing zone (BZ), or background (BG).

[b] Total number concentration (arithmetic mean ± standard deviation across SMPS scans) in the size range 14-663 nm, unless otherwise indicated.

[c] Arithmetic mean ± standard deviation across SMPS scans.

[d] On some days, we monitored more than one production run from a single sampling location. Values for each individual run are shown.

[e] The technician used a power drill to remove bits of the graphite rod from the reactor during this procedure.